

Zeitschrift: IABSE reports = Rapports AIPC = IVBH Berichte
Band: 73/1/73/2 (1995)

Rubrik: Session B2: Seismic strengthening: laboratory studies

Nutzungsbedingungen

Die ETH-Bibliothek ist die Anbieterin der digitalisierten Zeitschriften. Sie besitzt keine Urheberrechte an den Zeitschriften und ist nicht verantwortlich für deren Inhalte. Die Rechte liegen in der Regel bei den Herausgebern beziehungsweise den externen Rechteinhabern. [Siehe Rechtliche Hinweise.](#)

Conditions d'utilisation

L'ETH Library est le fournisseur des revues numérisées. Elle ne détient aucun droit d'auteur sur les revues et n'est pas responsable de leur contenu. En règle générale, les droits sont détenus par les éditeurs ou les détenteurs de droits externes. [Voir Informations légales.](#)

Terms of use

The ETH Library is the provider of the digitised journals. It does not own any copyrights to the journals and is not responsible for their content. The rights usually lie with the publishers or the external rights holders. [See Legal notice.](#)

Download PDF: 21.05.2025

ETH-Bibliothek Zürich, E-Periodica, <https://www.e-periodica.ch>



Session B2

Seismic Strengthening: Laboratory Studies
Renforcement parasismique: études de laboratoire
Seismische Verstärkung: Laborstudien

Leere Seite
Blank page
Page vide

Seismic Strengthening of Reinforced Concrete Columns with Inadequate Lap Splices

Renforcement parasismique de colonnes en béton armé
avec un recouvrement inadéquat des barres d'armature

Verstärkung von Stahlbetonstützen mit ungenügenden
Bewehrungsstößen gegen Erdbeben

Riyad S. ABOUTAHA

Assistant Professor
Georgia Inst. of Technology
Atlanta, GA, USA

Michael D. ENGELHARDT

Associate Professor
Univ. of Texas at Austin
Austin, TX, USA

James O. JIRSA

Professor
Univ. of Texas at Austin
Austin, TX, USA

Michael E. KREGER

Associate Professor
Univ. of Texas at Austin
Austin, TX, USA

SUMMARY

Results of an experimental investigation on the use of rectangular steel jackets for seismic strengthening of non-ductile rectangular reinforced concrete columns with inadequate lap splices in the longitudinal reinforcement are presented. The test columns were detailed with short lap splices and were lightly reinforced with transverse reinforcement. Columns were tested under cyclic lateral loads. The basic unretrofitted columns showed an early failure of the lap splices which resulted in dramatic loss of lateral strength and stiffness. The columns strengthened with steel jackets and adhesive anchor bolts showed excellent response, exhibiting higher strength, ductility and energy dissipation.

RÉSUMÉ

L'article présente les résultats d'une recherche sur l'emploi de manchons rectangulaires pour le renforcement parasismique de colonnes en béton armé avec un recouvrement inadéquat des barres d'armature longitudinales. Les colonnes-éprouvettes avaient de petits recouvrements d'armature et étaient légèrement renforcées transversalement. Les essais ont eu lieu pour des charges cycliques latérales. Les colonnes originales, non consolidées, ont rapidement présenté des dégâts, réduisant considérablement la résistance latérale et la rigidité de la colonne. Les colonnes consolidées par manchons métalliques et boulons d'ancrage collés ont présenté un comportement excellent, avec de grandes résistance, ductilité et dissipation d'énergie.

ZUSAMMENFASSUNG

Berichtet wird von Versuchen zur Blechummantelung von Stahlbetonstützen, deren Längsbewehrung erdbebenuntaugliche Ueberlappungsstöße aufweist. Teststützen mit kurzen Ueberlappungslängen und leichter Querbewehrung wurden zyklischer Horizontalbelastung unterworfen. Sie versagten frühzeitig an den Stößen, mit dramatischer Einbusse an seitlicher Steifigkeit und Festigkeit. Hingegen zeigten die mit Blechmantel und Klebedübel verstärkten Stützen ein hervorragendes Verhalten mit höherer Festigkeit, Duktilität und Energiedissipation.



1. INTRODUCTION

Older reinforced concrete columns were often designed primarily for gravity loads. Consequently, they were detailed as axially compression members, with lap splices in the longitudinal reinforcement proportioned as compression lap splices. However, during an earthquake, column bars may experience large tensile forces, which requires a longer well confined splice proportioned as a tensile lap splice. For ease of construction, column bars were often spliced just above floor levels, a potential hinge region, in columns, during an earthquake. Older columns were lightly reinforced with transverse reinforcement, which resulted in poorly confined lap splices. Being short, poorly confined and located in a potential plastic hinge region, older lap splices may cause failure of concrete columns during an earthquake. The current provisions of the ACI code 318-89 [1] allows splicing column longitudinal bars, only within the center half of the column, and if only proportioned as tension splices.

One possible method for strengthening columns with inadequate lap splices is the use of rectangular steel jackets. In this paper, results of an experimental research program, conducted at The University of Texas at Austin, on the use of rectangular steel jackets for seismic strengthening of rectangular concrete columns with inadequate lap splices in the longitudinal reinforcement are presented. Six large scale columns are reported, three were basic unretrofitted columns and the remaining three were retrofitted with steel jackets before testing. The major variables investigated in this series were the width of the column and the amount and distribution of adhesive anchor bolts.

2. TEST PROGRAM

2.1 Test Setup and Loading Program

Figure 1. shows the test setup. The test column is a cantilever specimen, representing the lower half of a real building column. Columns were laterally loaded at the tip of the column, but without axial load. The lateral loads were increased in 22 kN increments until significant inelastic displacement was observed. In the inelastic range the loading was increased in displacement increments equivalent to 0.5 % drift ratio. All the test columns were loaded in the weak direction.

2.2 Test Columns

The basic unstrengthened columns FC1, FC2 and FC3 were 915 mm, 686 mm and 457 mm wide, respectively. The corresponding strengthened columns were designated FC1S, FC2S and FC3S respectively. Figure 2. shows the details of the basic columns. The longitudinal bars were 25 mm in diameter. The transverse reinforcement was 9.5 mm in diameter spaced at 406 mm. Table 1. shows the properties of the test columns. All the longitudinal bars were spliced at the bottom of the column. The splice length was 610 mm which corresponds to 24 times the diameter of the bar. The test columns were detailed according to the provisions of the ACI 318-63 [2], which allows the use of a cross tie at every other longitudinal bar if the spacing between the main bars is less than 150 mm. The actual yield strength of the longitudinal bars and the transverse ties were 435 MPa and 400 MPa, respectively.

The retrofitted columns were similar to their corresponding basic columns, but were strengthened by the use of steel jackets and adhesive anchor bolts before testing. Figures 3, 4 and 5 show the details of the retrofitted columns FC1S, FC2S and FC3S, respectively. The sides of the steel jacket were made of 6 mm steel plates and the corners of the steel jacket were 50x50x6 mm steel angles which were welded to the steel plates. All the steel jackets had similar details with the exception of the steel jacket of column FC3S, which had four additional 75x75x6 mm angles, as shown in Figure 5. These additional angles were welded to the steel jacket after the setting of the non-shrink grout. The actual yield strength of the steel plates was 345 MPa. Since the concrete column section was quite symmetrical about the weak axis, two different patterns of anchor bolts were installed on the opposite faces of

the column, as shown in Figures 4 and 5. The steel jackets extended over the bottom 915 mm of the column height, which corresponded to 1.5 times the length of the splice.

The steel jackets were pre-fabricated in two L-shaped panels in plan, as shown in Figure 6. The two opposite free ends of the steel jacket were welded after being assembled around the column. The 25 mm gap between the concrete column and the steel jacket was filled with non-shrink cementitious grout. The adhesive anchor bolts were 25 mm in diameter and 300 mm in length. Bolts were installed in pre-drilled holes using an adhesive compound, and were embedded 200 mm into the concrete column.

Column #	Size (width* depth) (mm)	Main Bars (number-Diameter)	Transverse Ties (number-diameter)	Concrete Strength (MPa)*	Grout Strength (MPa)*	Bolts** East Side	Bolts ** West Side	Description
FC1	915x457	16-25mm	5-9.5mm	19.7	----	----	----	basic
FC2	686x457	12-25mm	4-9.5mm	28.7	----	----	----	basic
FC3	457x457	8-25mm	2-9.5mm	28.7	----	----	----	basic
FC1S	915x457	16-25mm	5-9.5mm	22.5	43.2	2L3B	2L2B	strengthened
FC2S	686x457	12-25mm	4-9.5mm	17.7	38.6	1L2B	None	strengthened
FC3S	457x457	8-25mm	2-9.5mm	18.1	51.3	None	None	strengthened

* Strength at the day of Testing. ** L = Vertical Line(s), B = Adhesive Anchor Bolts. Example: 2L3B = 2 lines of anchor bolts; each line with 3 bolts.

Table 1 Properties of the test columns

3. TEST RESULTS

Figure 7 (a-f) shows the hysteretic response of the test columns. As shown in Figure 7 (a-c) the basic unretrofitted columns exhibited non-ductile flexural response. Lap splice failure occurred before the development of the flexural capacities of the columns. The splice failure was always associated with vertical splitting cracks along the full length of the splice. After splice failure, the columns rapidly lost lateral strength and stiffness. All the basic unretrofitted columns showed essentially no ductility and very limited energy dissipation.

The retrofitted columns exhibited very satisfactory response, as shown in Figure 7 (d-f). Both sides of column FC1S performed very well, and the flexural capacity was developed without any lap splice failure. The response of column FC1S suggests that just two adhesive anchor bolts near the top and two near the bottom of the jacket are sufficient for strengthening 915 mm wide columns with inadequate lap splices. However, for narrower columns fewer bolts are required, as indicated by the results of columns FC2S and FC3S. Welding the additional four angles on the steel jacket of column FC3S after the setting of the non-shrink grout appeared to develop some tensile residual stresses in the steel jacket. The tensile residual stresses provided active confinement for the splice region, which resulted in high energy dissipation. Additional details on the performance of the reported columns can be found in reference [3].



4. SUMMARY

Six large scale columns with inadequate lap splices in the longitudinal reinforcement were investigated under cyclic lateral loads. Columns were tested with and without rectangular steel jackets. The details and the cyclic response of the columns were presented. Test results suggest that rectangular steel jackets with adhesive anchor bolts are very effective in strengthening columns with inadequate lap splices. For the narrower column tested in this program (457 mm width), a plain steel jacket without anchor bolts significantly improved its seismic response.

REFERENCES

1. ACI Building Code Requirements for Reinforced Concrete (ACI 318-89), American Concrete Institute, Detroit, Michigan, 1989.
2. ACI Building Code Requirements for Reinforced Concrete (ACI 318-63), American Concrete Institute, Detroit, Michigan, 1963.
3. Aboutaha, Riyadh S. "Seismic Retrofit of Non-Ductile Reinforced Concrete Columns Using Rectangular Steel Jackets," Ph.D. Dissertation, The University of Texas at Austin, Austin, Texas, 1994.

ACKNOWLEDGMENTS

The writers gratefully acknowledge the financial support provided by The National Science Foundation (Grant No. BCS - 9016828). This project is part of the NSF program on Repair and Rehabilitation Research for Seismic Resistance of Structures. Additional support was provided through NSF Grant No. CMS-9358186. The writers also thank Loring A. Wyllie Jr. and Thomas A. Sabol for providing many useful suggestions and comments during the course of this project. Thanks are also extended to Hilti Inc. for donating the adhesive anchor bolts and construction tools used in this research.

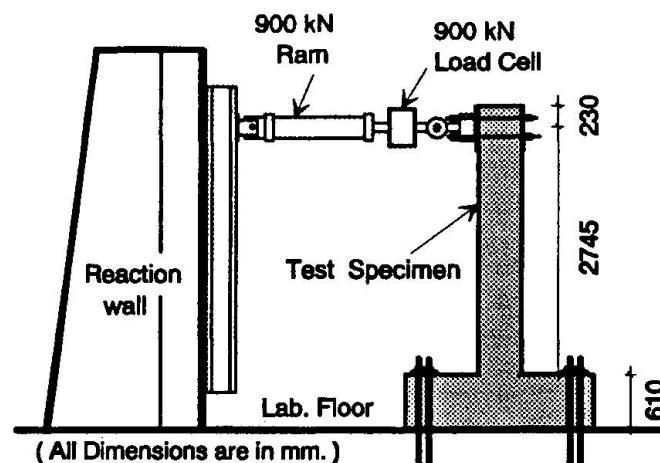


Fig.1 Test Setup

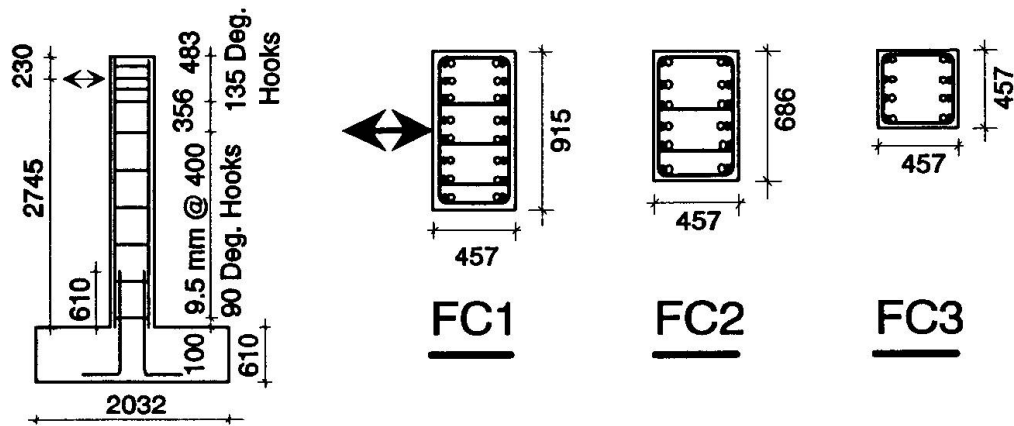


Fig. 2 Basic Unretrofitted Columns FC1, FC2 and FC3

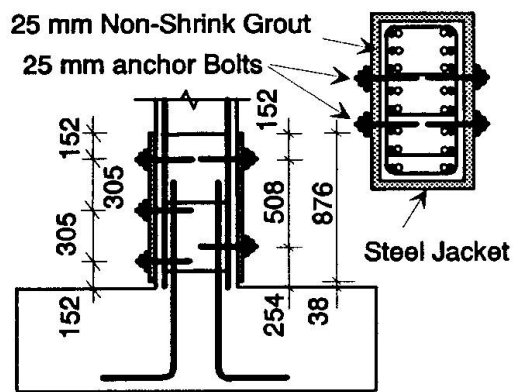


Fig. 3 Strengthened Column FC1S

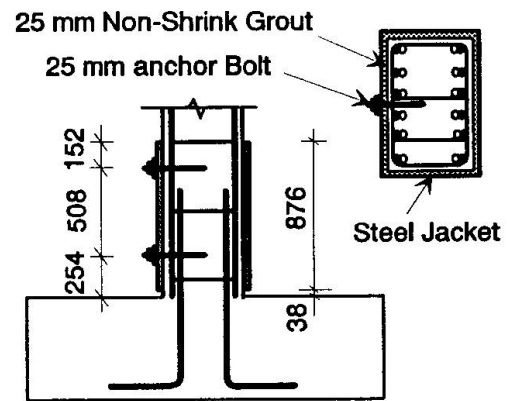


Fig. 4 Strengthened Column FC2S

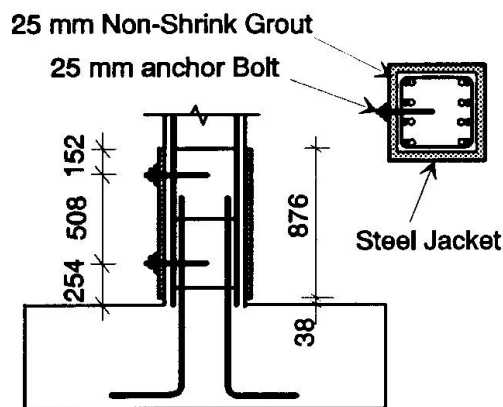


Fig. 5 Strengthened Column FC3S

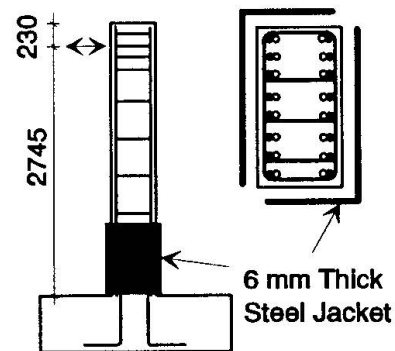
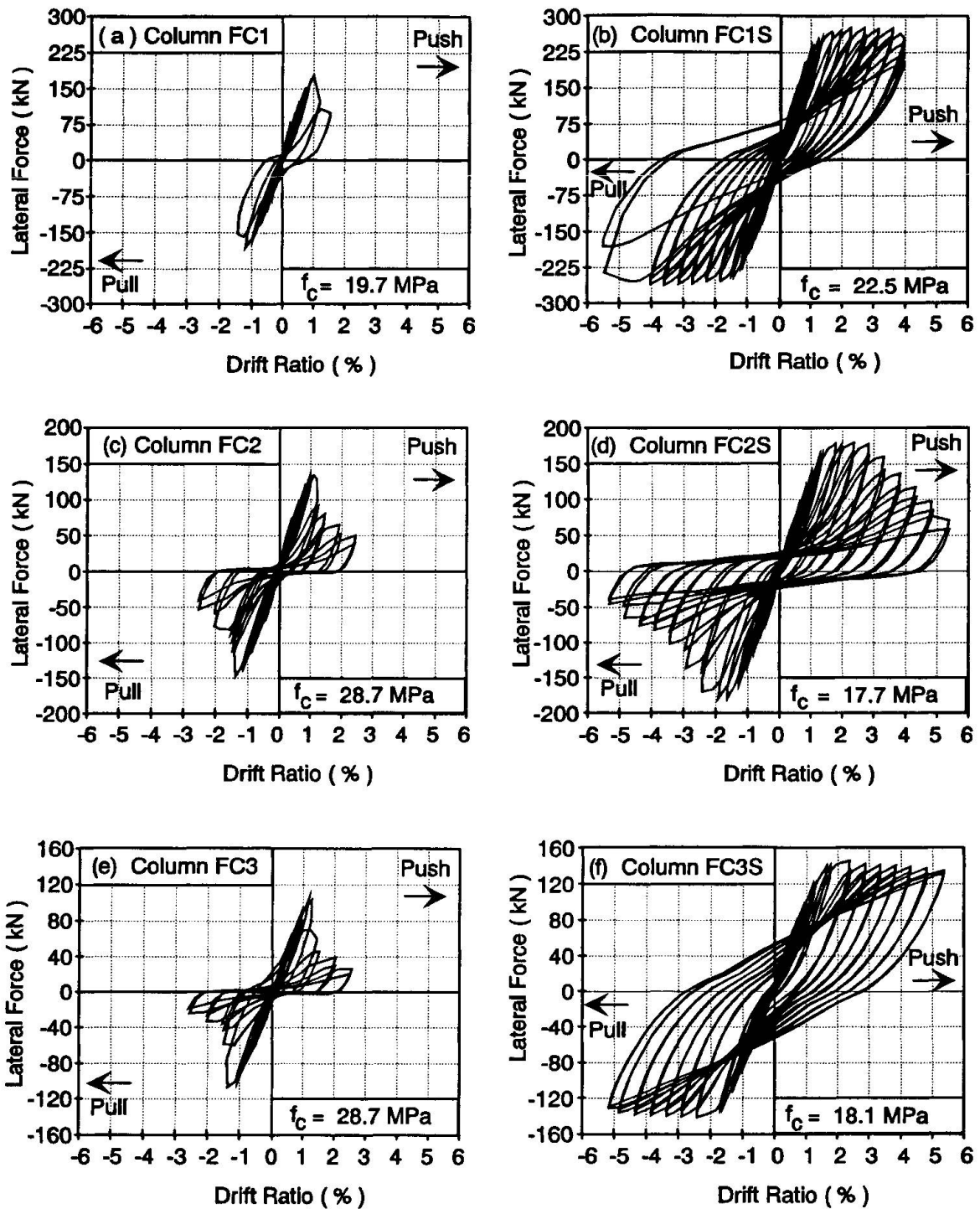


Fig. 6 Assembling of Steel Jacket



Basic Unretrofitted Columns

Strengthened Columns

Fig. 7 (a-f) The hysteretic response of the test columns

High-Strength Concrete Beam-Column Joints under Seismic Loading

Noeuds de cadres en béton à haute résistance sous charges sismiques

Rahmenknoten aus hochfestem Stahlbeton unter Erdbebenbelastung

Ahmed M. YOUSEF

Dr. Eng.
Univ. for Arch. and Civil Eng.
Sofia, Bulgaria



Ahmed M. Yousef, born 1961, received his B.Sc. and M.Sc. in Structural Engineering at the Faculty of Engineering, El-Mansoura University, Egypt, where he is working, as assistant lecturer. Since June 1992, he is pursuing his study towards the Ph.D. degree at Sofia University.

Ivan YAKIMOV

Associate Professor
Univ. for Arch. and Civil Eng.
Sofia, Bulgaria



Ivan Yakimov, born 1935, is Associate Professor at the Department of Concrete Structures, Univ. for Architecture and Civil Engineering, Sofia, Bulgaria. His research activities are in the area of reinforced and prestressed concrete structures, as well as composite construction design.

SUMMARY

The results from reversed cyclic loading tests on six exterior beam-column joints constructed with high strength concrete are presented. Three of the tested specimens were reinforced with crossed inclined bars within the joint core instead of the intermediate vertical column bars. The primary variables were the percentage of the transverse reinforcement in the joint, the amount of crossed reinforcement bars and the ratio of the column-to-beam flexural capacity. The results showed an excellent joint behaviour.

RÉSUMÉ

L'article présente les résultats de recherches expérimentales sur six éprouvettes de noeuds de cadres réalisés en béton à haute résistance, soumis à un chargement cyclique. Trois éprouvettes ont été armées avec des barres inclinées et croisées au noyau de noeud, au lieu de barres centrales longitudinales de la colonne. Les premières quantités variables étaient la section transversale des barres inclinées et le pourcentage de l'armature transversale au noeud. Les résultats ont montré un comportement excellent de toutes les éprouvettes.

ZUSAMMENFASSUNG

Die Forschungsergebnisse für 6 Probekörper von externen Rahmenknoten unter zyklischer Belastung, die aus hochfestem Beton hergestellt worden waren, werden vorgestellt. Drei von diesen Probekörpern waren statt gerader Längsstäbe in der Säule mit geneigten kreuzenden Längsstäben im Rahmenknotenkorbe bewehrt. Die Querschnittfläche der kreuzenden Längsstäbe, das Prozent der Querbewehrung im Rahmenknotenkorben und das Verhältnis der Säule- und Balkentragfähigkeiten waren die ersten Variablen. Die Ergebnisse haben ein vorzügliches Verhalten des Rahmenknotens gezeichnet.



1. INTRODUCTION

Guidelines for designing beam-column joints of reinforced concrete ductile moment resisting frames were recommended by ACI-ASCE Committee 352 [1]. The design provisions stipulated in chapter 21 of ACI 318-89 (revised 1992) building code [2] were largely based on the work of the committee 352. Tests providing the basic data for these provisions were conducted on connections with concrete compressive strength (f_c) mostly less than 40 MPa. With the commercial availability of high strength concrete (HSC) with compressive strengths approaching 120 MPa [3], many questions have been raised regarding the applicability of these design provisions for HSC.

The 352 recommendations require a minimum flexural strength ratio at the joint (M_R) of 1.4 and a maximum allowable joint shear stress in the form of $\gamma \sqrt{f_c}$, where joint shear stress factor γ is a function of the joint type and the loading conditions. The required joint transverse reinforcement, which is calculated independently of these two variables, can cause congestion of the joint especially when using HSC. The reported studies on the seismic behaviour of HSC beam-column joints showed that these joints have sufficient energy dissipating capacity and load carrying capacity [4],[5]. On another hand, Tsonos, Tegos, and Penelis [6] suggested the use of crossed inclined bars within the joint core in order to improve the performance of Type 2 exterior beam-column joints.

The main objectives of this experimental study were to investigate the effect of joint transverse reinforcement on the seismic behaviour of exterior beam-column joints constructed with HSC (f_c varied between 69 and 77 MPa) and to examine the efficiency of using inclined reinforcing bars within the joint core as a method of reducing the quantity of joint transverse reinforcement required by the ACI-ASCE Committee 352.

2. TEST PROGRAM

2.1 Test Specimens

Six reinforced concrete beam-column subassemblies were constructed with HSC. According to the classification of the 352 recommendations, the configuration of the specimens qualifies them as corner joint. all specimens were cast flat. After the reinforcing cage was placed into the form, concrete was placed and internally vibrated. The specimens were removed from the form after seven days and were moist-cured for 28 days. The minimum age of the specimens at the time of testing was four months.

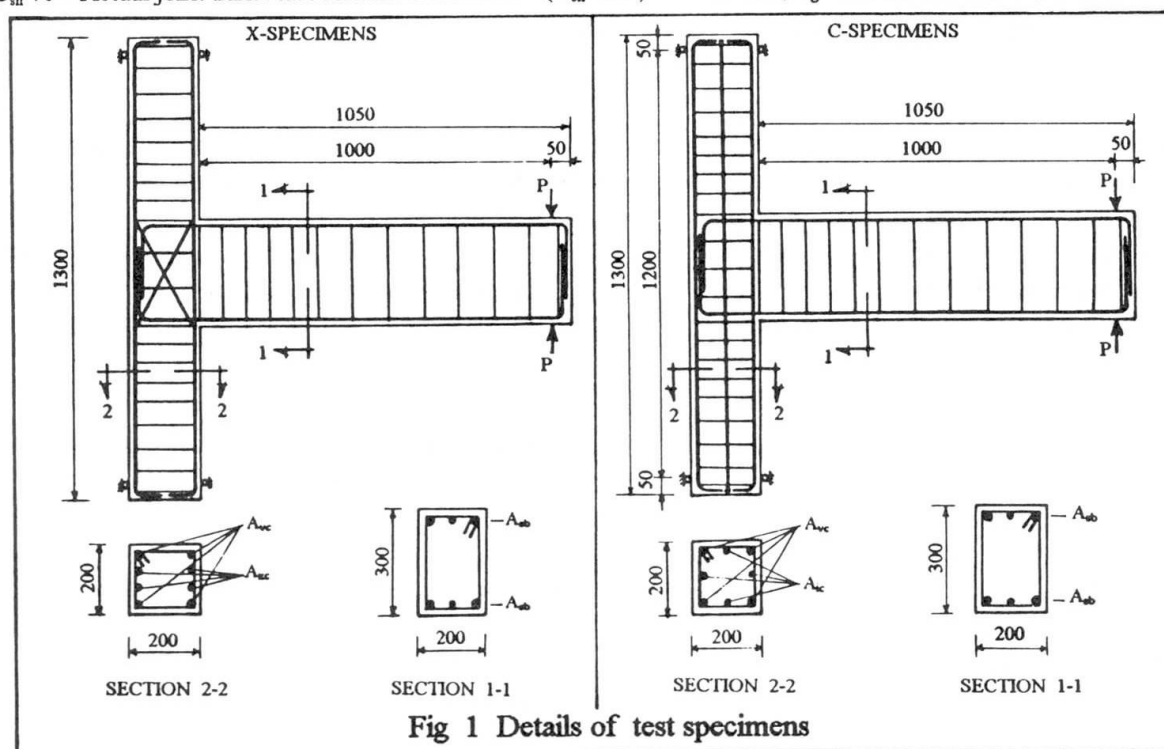
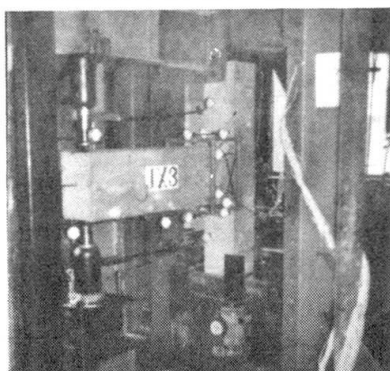
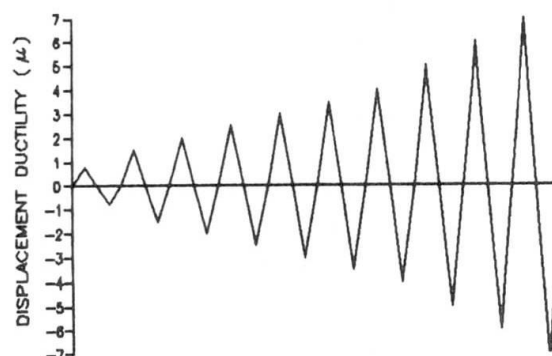
All specimens have the same dimensions in three series. Each of them consists of two specimens, one conventionally reinforced in the joint region (C-Specimens) and one specimen reinforced with inclined crossed bars (X-Specimens) as shown in Fig. 1. The specimens of each series differed only in reinforcement details at the joint region as given in Table 1. The X-Specimens were reinforced with four crossed inclined bars bent diagonally across the joint core as shown in Fig.1, instead of the four intermediate longitudinal bars in the columns of the X-Specimens. In addition, the joint transverse reinforcement of the second specimen of each series was always less than that of the first one. For all specimens, the transverse reinforcement in the joint was extended to the column at 50 mm spacing. The beam shear reinforcement included R8 rectangular hoops with a 135-deg standard hook. The maximum allowable spacing being one-fourth of the beam effective depth according to the seismic provisions of ACI Building Code [2].

According to the 352 recommendations, the maximum joint shear stress for a corner joint constructed with ordinary strength concrete is ($0.083 \gamma \sqrt{f_c}$ MPa) where joint shear stress factor γ is equal to 12, and the concrete compressive strength f_c was limited to 41 MPa. The design shear stress factor of the specimens was kept below 12 as given in Table 1. The joint shear stresses were calculated when the specimens were designed assuming that strain hardening will increase the tensile strength in the beam longitudinal reinforcement by 15% over the measured tensile yield strengths. The recommendations set a lower limit of 1.4 for the flexural strength ratio (M_R), defined as the

Table 1 Summary of test program

Specimens	f_c (MPa)	A_{sb}	A_{vc}	A_{ic}	A_{xc}	Joint hoops	$\rho_{sh}\%$	$\rho_{ACI}\%$ Eq. (1)	$\rho_{ACI}\%$ Eq. (2)	M_R	γ	$N/f_c A_g$
JC1	73.3	2D14	4D12	4D10	-	3R6/3	0.71	4.8	2.5	1.4	6.2	0.15
JX1	77.1	2D14	4D12	-	4D10	3R6	0.47	5	2.7	1.4	6.2	0.15
JC2	71.1	2D14 +1D10	4D14	4D12	-	2R8/3	0.94	3.8	2	1.4	8.1	0.06
JX2	69.2	2D14 +1D10	4D14	-	4D12	2R8	0.63	3.7	2	1.4	8.1	0.06
JC3	69	2D14	4D16	4D14	-	3R6	0.47	4.5	2.4	2.4	6.2	0.15
JX3	69.7	2D14	4D16	-	4D14	2R6	0.35	4.5	2.4	2.4	6.2	0.15

Note: © D10, D12, D14, D16=Deformed bars with yield strength $f_y = 532.9, 397.6, 446.1, \text{ and } 392.1$ MPa respectively.
 © R6, R8=Plain bars with diameters 6, 8 mm, $f_y = 260.3, 315.6$ MPa respectively. © 3R6/3=Three hoops with cross-ties.
 © $\rho_{sh}\%$ = Actual joint transverse reinforcement ratio = (A_{sh}/sh) © $N/f_c A_g$ = Axial load intensity Index.


Fig 1 Details of test specimens

Fig 2 General view of loading setup

Fig 3 Cyclic load sequence used in the tests



sum of the flexural capacities of the columns to that of the beam at the connection region. For the tested specimens, M_R was equal to 1.4 or 2.4.

In order to insure adequate confinement of the joint core, the recommendations require that the total cross-sectional area of hoops and crossties A_{sh} to be calculated from the following equations:

$$A_{sh} = 0.30 sh'' (f_c / f_{yh}) (A_g / A_c - 1) \quad (1)$$

but not less than $A_{sh} = 0.09 sh'' (f_c / f_{yh}) \quad (2)$

where A_{sh} = total cross-sectional area of hoops and crossties in each set; A_g = gross area of column section; A_c = area of column core bound by stirrups; f_c = compressive strength of concrete cylinder; f_{yh} = yield strength of stirrups; h'' = core dimension of the column; and s = spacing of stirrups.

Satisfying these requirements results in joints that are congested with reinforcement and impractical to construct. For all specimens, the joint transverse reinforcement ratio ρ_{sh} was kept well below the requirements of the Committee 352 as shown in Table 1.

For all the six specimens, the terminating beam longitudinal bars were hooked within the transverse reinforcement of the joint using 90 deg standard hook. Due to the lack of data about the required development length in HSC, the required length was calculated using the equation recommended by the Committee 352 for ordinary strength concrete. The provided length measured from the critical section defined by the recommendations was little less than that required (about 135 mm).

2.2 Materials

A concrete mix using ordinary portland cement and limestone coarse aggregate with maximum dimension of 12 mm was used. The mix proportions for 1 m³ of concrete consisted of 545 kg cement, 55 kg fly ash, 1100 kg coarse aggregate, 635 kg sand, 165 kg water and 20 liter superplastizer. The slump of the mix was approximately 55 mm. The average cylinder concrete compressive strength after 28 days for each specimen is presented in Table 1. The minor difference in concrete compressive strength was assumed to have no significant influence on the test results.

2.3 Loading Setup and Instrumentation

The specimens were tested with the column portions placed vertically in the steel frame as shown in Fig. 2. An axial load was applied to the column and kept constant throughout each test as given in Table 1. The free ends of the beams were subjected to several slow load reversals simulating very severe earthquake loading by two 120 KN hydraulic jacks. The typical loading sequence is shown in Fig. 3. The first cycle was load controlled in the elastic range up to 75% of the theoretical flexural strength of the beam, as calculated on the basis of the measured material strengths, and was followed by a series of deflection controlled cycles in the inelastic range until a displacement ductility factor (μ) equal to 7. Approximately 36 electrical strain gauges were bonded to the reinforcing steel at the critical locations near and within the joint region of each specimen. In addition, sufficient instrumentation was provided to monitor the deflections of the beam and the deformations in the potential plastic hinge region.

3. DISCUSSION OF TEST RESULTS

3.1 General Performance and Effect of Inclined Bars

The overall behaviour of the specimens is best described by plots of the applied load versus the displacement of the beam at the load point as shown in Fig. 4. All the HSC specimens exhibited excellent ductile hysteretic response until the loading was terminated at storey drift equal to 4.9% ($\mu=6$) for specimens JC2 and JX2, and 4.2% ($\mu=7$) for specimens JC1, JX1, JC3, JX3. The flexural strength ratio M_R of the specimens was equal to 1.4 or more as required by the 352 Committee. Therefore, all the specimens failed due to flexural hinging at the end of the beam. Only

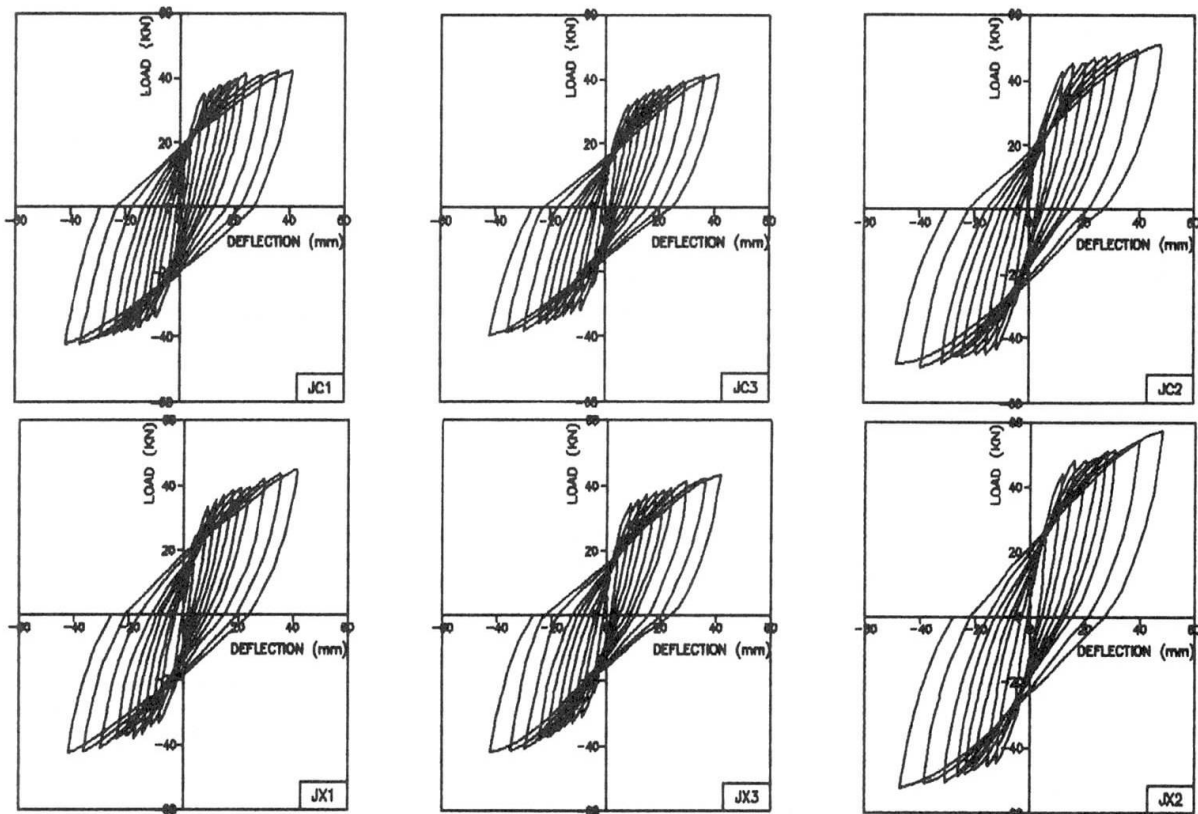


Fig. 4 Load-displacement response for the specimens

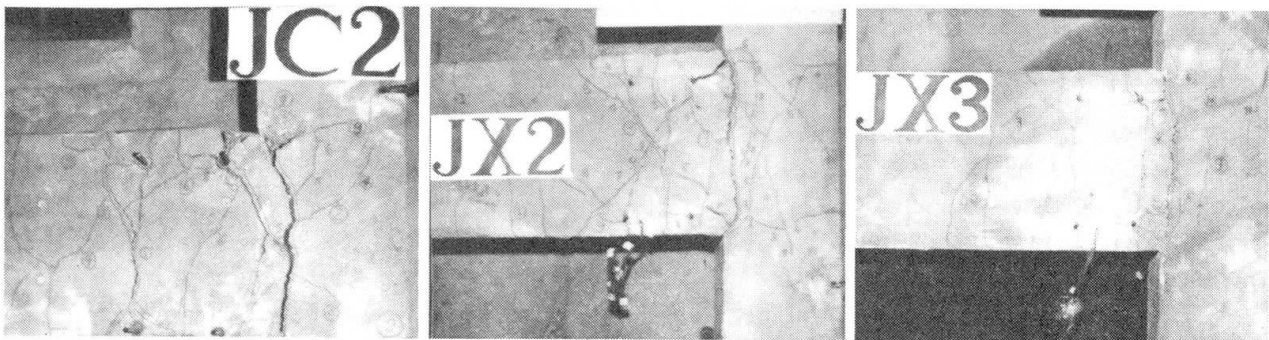


Fig. 5 Cracking in the joint region for three specimens at the end of the test

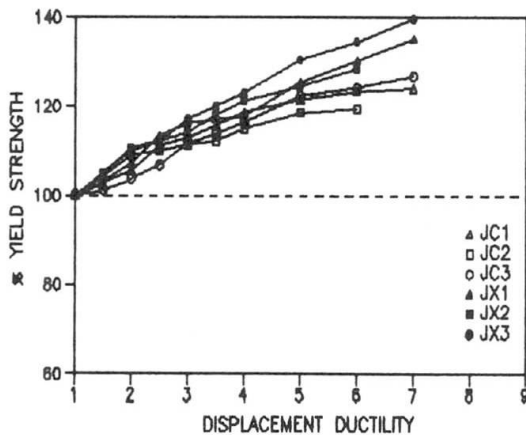


Fig. 6 Cyclic load-carrying capacity of the specimens

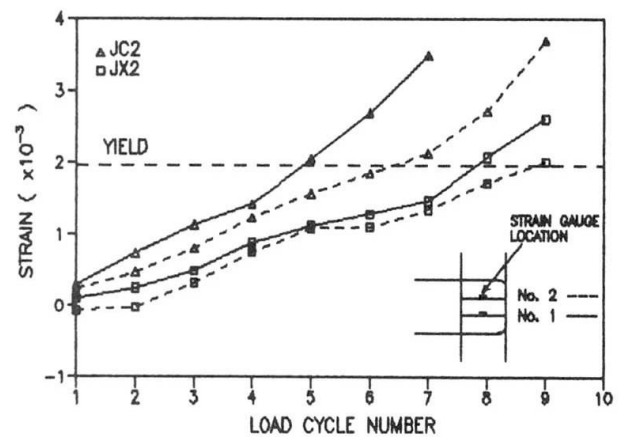


Fig. 7 Maximum strain in joint core hoops of specimens JC2 and JX2 during the positive loading runs of each cycle



minor cracking occurred in joint region for specimens JC1, JX1, JC3, and JX3, while in specimens JC2 and JX2, which had the largest joint shear stress, there were many more and larger cracks as shown in Fig. 5. In order to compare the performance of X-Specimens and C-Specimens a plot of percent yield strength versus the displacement ductility is shown in Fig. 6. The yield load and displacement for each specimen were measured from the strain gauge data of the beam longitudinal reinforcement at the face of the column. The presence of inclined crossed bars within the joint core of X-Specimens enhanced its load carrying capacity by more than 10% compared with that of C-Specimens. Specimen JX2 with 4D12 inclined bars had less load carrying capacity than JC2 with 4D10 inclined bars. This showed that increasing the amount of inclined bars had a significant improvement when the joint shear stress was low.

3.2 Effect of Joint Transverse Reinforcement

The required joint transverse reinforcement using Eq. (1) and Eq. (2), as recommended by the committee 352, is linearly proportional to f_c . For joints constructed with HSC ($f_c > 50$ MPa), these equations lead to very large amounts of confinement steel, as shown in Table 1, and it is practically impossible to construct a joint with such amount of stirrups. For the C-Specimens, $\rho_{sh} \approx 0.2$ to 0.5 of ρ_{ACI} required by Eq. (1). However, all C-Specimens behaved very satisfactory. Plots of strains measured on the joint stirrups for specimens JC2 and JX2 is shown in Fig. 7. Yielding of the joint hoops and crossies was recorded from cycle 5 onwards (from $\mu=3$). However, in none of the specimens did the cover concrete of the back of the column opposite to the beam separate from the joint core. The tests showed that the major part of joint shear was resisted by the diagonal compression strut even after severe load reversals, and using HSC increased proportionally its strength. Fig. 7 demonstrates that the hoops of C-Specimens accepted more tension than that of X-specimens despite the fact that C-Specimens had greater amount of joint hoops. This was because the crossed inclined bars accepted more shear stress than the intermediate longitudinal column bars.

4. CONCLUSIONS

From the results of this experimental study, the following can be concluded:

1. Exterior beam-column joints constructed with high-strength concrete ($f_c = 69$ to 77 MPa) showed excellent ductile behaviour up to 4.9% storey drift.
2. The minimum amount of transverse reinforcement required by the ACI-ASCE Committee 352 recommendations for Type 2 HSC exterior beam-column joints may be safely reduced by at least 50%, for the cases with $\gamma < 12$ in combination with $M_R \geq 1.4$, without loss of ductility requirements.
3. Exterior beam-column joints with crossed inclined reinforcing bars performed considerably better than those with conventional reinforcement. The presence of inclined reinforcing bars within the joint core also resulted in a reduction of the joint transverse reinforcement to only about 33% of the requirements of the Committee 352 recommendations.

REFERENCES

1. ACI-ASCE Committee 352, Recommendations for Design of Beam-Column Joints in Monolithic Reinforced Concrete Structures, ACI 352R-91, 1991.
2. ACI Committee 318, Building Code Requirements for Reinforced Concrete (ACI 318-89 revised 1992), American Concrete Institute, Detroit, 1992.
3. ACI Committee 363, State-of-the-Art Report on High-Strength Concrete, ACI 363R-92, 1992.
4. EHSANI M. R., MOUSSA A. E., and VALLENILLA C. R., Comparison of Inelastic Behaviour of Reinforced Ordinary-and High-Strength Concrete Frames, ACI Structural J., March-April 1987.
5. SUGANO S., NAGASHIMA T., KIMURA H., and ICHIKAWA A., Behaviour of Beam-Column Joints using High-Strength Materials, ACI SP-123, 1991.
6. TSONOS A. G., TEGOS I. A., and PENELIS G. GR., Seismic Performance of Type 2 Exterior Beam-Column Joints Reinforced with Inclined Bars, ACI Structural J., Jan.-Feb. 1993.

Behaviour of Strengthened Reinforced Concrete Beam-Column Joints

Comportement des noeuds de cadres en béton armé après consolidation
Verhalten von Stahlbetonrahmenknoten nach Verstärkung

Longmei SHENTU
Lecturer
Tongji University
Shanghai, China



Longmei Shentu, born in 1965, received his Master's degree of engineering at Tongji University. For six years, he was involved not only in the design of reinforced concrete structures, but in research and design of projects related to structural strengthening as well. His research interests also include finite element analysis.

SUMMARY

Based on the simulation of existing reinforced concrete beam-column joints in which seismic loads have not been considered in design or whose seismic strength is not adequate, this paper presents an experimental investigation of different strengthening methods with externally glued steel. Using the pseudo-dynamic test method, two sets of specimens including a total of seven specimens are presented. Strengthening methods were developed to improve the shearing strength at the cores, while two further methods are presented to strengthen the positive flexural strength at the beam ends. The experimental results show that joints properly strengthened with glued steel can exhibit greatly enhanced seismic performance.

RÉSUMÉ

L'auteur présente différentes méthodes de renforcement par collage de tôles d'acier à l'extérieur des noeuds de poutres-cadres en béton armé, qui ont été à l'origine insuffisamment dimensionnés sous charge sismique. Il examine les essais pseudodynamiques effectués sur sept échantillons. Il expose des procédés de renforcement pour augmenter la résistance au cisaillement des noeuds, ainsi que pour augmenter la résistance à la flexion des jonctions montants-traverses de ces cadres, cette consolidation étant réalisée à l'aide de tôles d'acier collées. Les résultats expérimentaux montrent que les noeuds correctement renforcés offrent des performances sismiques nettement plus élevées.

ZUSAMMENFASSUNG

Der Beitrag behandelt unterschiedliche Verstärkungsmethoden für Stahlbetonrahmenknoten, bei deren Bemessung Erdbebenbelastung unzureichend berücksichtigt wurde. In pseudodynamischen Versuchen wurden insgesamt sieben Prüfkörper in zwei Serien untersucht. Drei Verstärkungsmethoden wurden für die Erhöhung der Schubtragfähigkeit im Knotenkern entwickelt, zwei weitere für die Erhöhung der Biegetragfähigkeit der Riegelanschlüsse. Verwendet werden extern aufgeklebte Stahlbleche. Die Versuchsergebnisse belegen, dass Knoten mit richtig angebrachten Stahlverstärkungen ein deutlich erhöhtes seismisches Leistungsvermögen aufweisen.



1. INTRODUCTION

With advantages such as fast construction, less additional weight, and only minor changes in the shapes of the beams, the strengthening of reinforced concrete beams with externally glued steel plates has been successfully utilized in many projects.

Seismic behavior of reinforced concrete beam-column joints has been broadly studied, which has greatly improved the seismic design in the RC structures. In existing buildings, however, there are many cases in which the structures were designed without considering the seismic loads or the existing seismic strengths will not be strong enough to withstand newly predicted major seismic events. In some cities such as Shanghai in China, the new provisions of seismic design demand higher seismic strengths than were standard, and many important buildings have to be strengthened to meet the new provisions. In these cases, the cores in a RC frame usually could bear only small shearing forces and the beam ends could hardly bear any positive moments although they usually could bear negative ones. It would be practical to employ the strengthening method of externally glued steel plates to improve the seismic performance of these structures.

The cyclic behavior of the bond between concrete and steel plate had been tested [1] to be sure that the glued steel plate could work well with the concrete beam under cyclic loads. Subsequently seven specimens of beam-column joints were tested, using five different strengthening methods. The experimental results of these tests are presented in this paper.

2. TEST SPECIMENS AND EXPERIMENTAL MODEL

Though in practice it is usual that both cores and beam ends need to be strengthened, separated strengthening methods were adopted in these tests, in which only the cores (SET I) or the beam ends (SET II) were strengthened to clearly investigate the difference between the strengthening methods. The seven specimens had the same size having the columns 1,910mm long and cross sections 200mm wide and 250mm deep, and the beams also 1,910mm long, which included the column depth, and their cross sections 120mm wide and 250mm deep.

In SET I, four specimens, which are identified as J1, J1G1, J1G2 and J1G3 were tested. Each specimen had longitudinal steel reinforcement consisting of one 16mm-diameter deformed bar at each corner of the beam and the column while the shear reinforcement consisted of 6mm-diameter stirrups at 100mm spacing, except the joint core where no transverse bars were provided. Therefore, the seismic load that the column and the beam could bear was much bigger than that of the core. If there are no longitudinal beams between reinforced concrete frames, it is possible to glue steel plates along both lateral surfaces of the beams such as J1G1 shown in Fig. 1a, in which the glued steel plates will act just as the transverse bars within the cores. However, longitudinal beams are usually provided to strengthen the stability of frames along the longitudinal direction and make the strengthening method of J1G1 impossible, thus a new strengthening method was developed in J1G2, in which four pieces of 40x4mm angle steel were glued at the column corners and they were connected by closed ties of steel plates at 100mm spacing, except the area of the beam depth. In order to greatly confine the core, another four pieces of the same size angle steel were provided to strengthen the lateral rigidity of the former angle steel as shown in Fig 1.b. The difficulty with this strengthening method is that the slab at column corners must be punched to let the angle steel go through. To avoid this inconvenience in construction, the strengthening method J1G3 shown in Fig 1.c was developed. A comparison with J1G2, in which the only difference was that the angle steel in J1G3 was cut in the place of the imaginary slab, could now be drawn.

In SET II, three specimens identified as J2, J2G1 and J2G2 were tested. The column of every specimen in this set was provided with four 16mm-diameter longitudinal deformed bars, while the beam had two 16mm-diameter bars on top and two 12mm-diameter plain steel bars at the bottom. The transverse steel bars in both the column and the beam consisted of 6mm-diameter stirrups at the space of 100mm while five 10mm-diameter plain steel stirrups were provided within the core. Since the purpose in this set was to find a way of improving the flexural strength at beam ends during seismic events, the flexural strength at beam ends was the only item that needed to be strengthened. If there are longitudinal beams, the

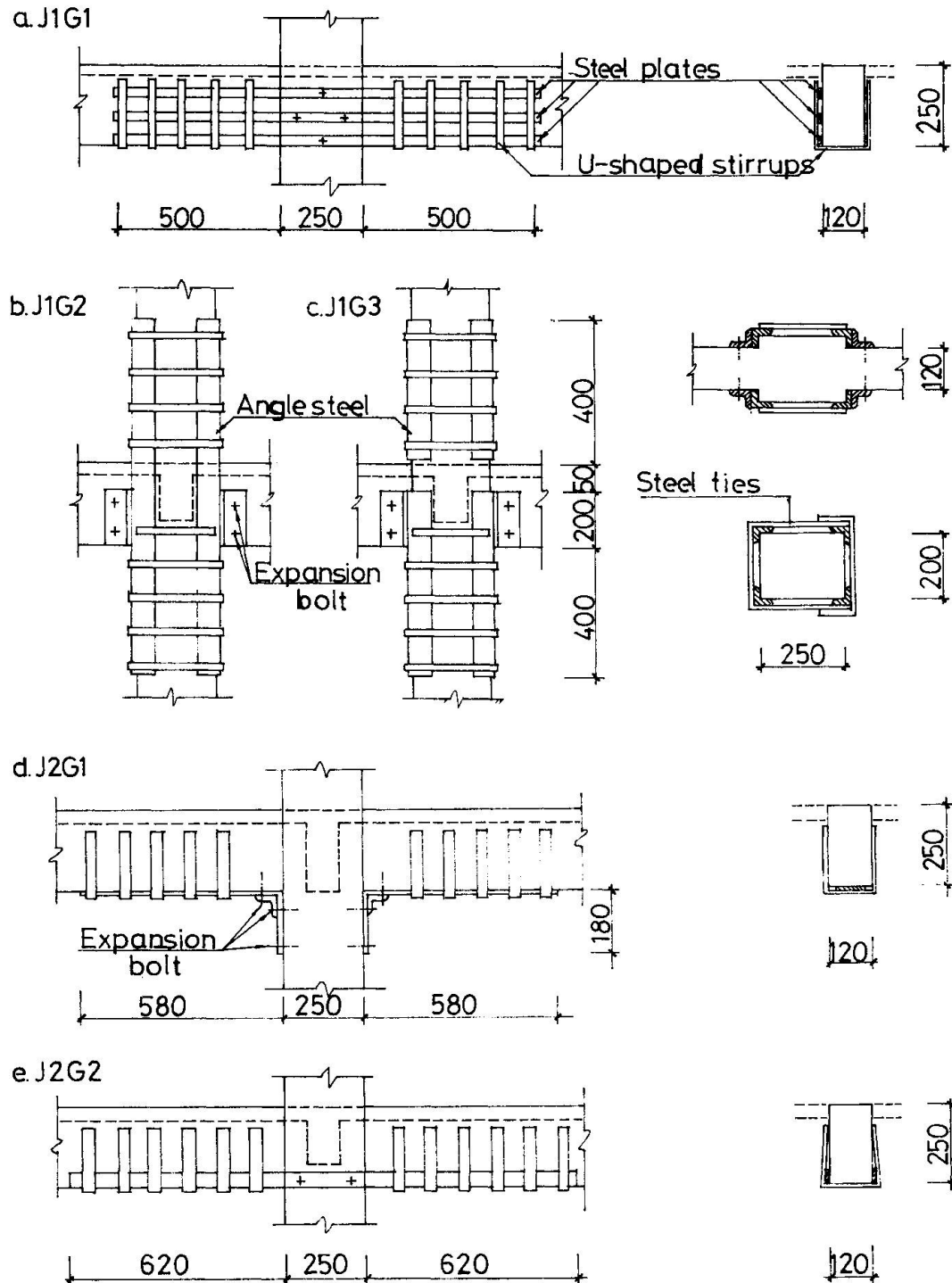


Fig. 1 Strengthening methods

depth of which is less than that of frame beams, it is possible to glue steel plates on the lateral surfaces of the frame beams as shown in Fig 1.e (J2G2). However, when the depth of the longitudinal beams is the same as or very near to that of the frame beams, it is impossible for the joints to be strengthened as in J2G2. Another strengthening method shown in Fig 1.d (J2G1) was developed where the steel plate was glued on bottom surface of the beam and bent vertically when it approached the column, and a piece of angle steel was used to strengthen the anchorage between the plate and the column. Both J1 and J2 which remained unstrengthened were used for comparison. And the properties of the materials used in the experiments are shown in Table 1.



Since these tests concentrated on the improvement of the shearing strength at the cores and the flexural strength at the beam ends under seismic loads, the effect caused by the lateral displacement at tops of the columns was relatively minor. The experimental model used is shown in Fig.2, in which the cyclic loads were antisymmetrically acted at the two free ends of the beam, while a constant vertical load was acted at the column ends where the lateral displacements were restrained.

Materials		Yield strengths (MPa)	Ultimate Strengths (MPa)
Steel bars	$\phi 6$	218	394
	$\phi 10$	293	461
	$\phi 12$	238	392
	$\phi 16$	361	568
Steel plate	$t=2\text{mm}$	308	430
	$t=3\text{mm}$	256	335
Concrete		$f_c=18.54\text{ MPa}$	

Table 1. Properties of materials

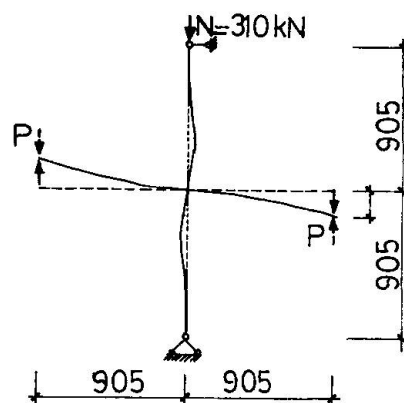


Fig.2. Experimental model

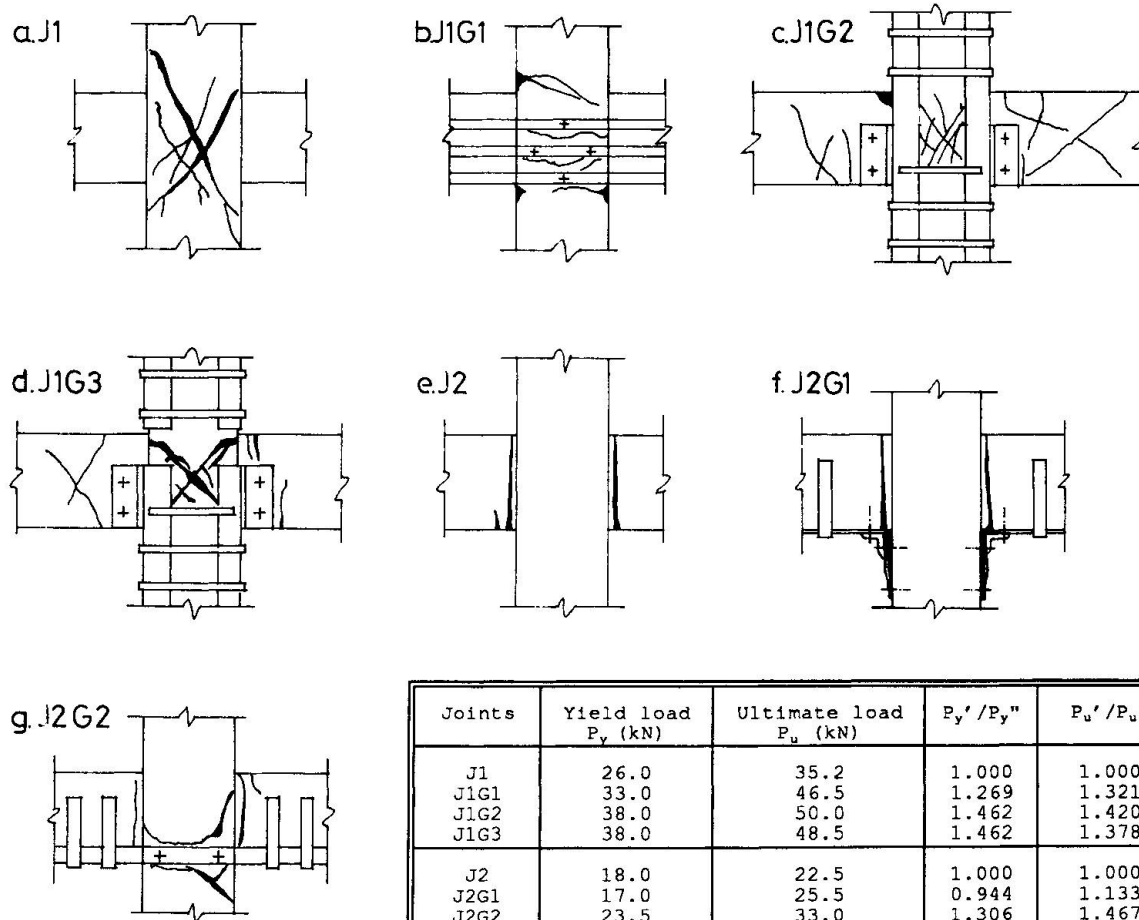


Fig.3. Failure of specimens

Joints	Yield load P_y (kN)	Ultimate load P_u (kN)	P_y'/P_y''	P_u'/P_u''
J1	26.0	35.2	1.000	1.000
J1G1	33.0	46.5	1.269	1.321
J1G2	38.0	50.0	1.462	1.420
J1G3	38.0	48.5	1.462	1.378
J2	18.0	22.5	1.000	1.000
J2G1	17.0	25.5	0.944	1.133
J2G2	23.5	33.0	1.306	1.467

P_y' , P_u' :strengthened; P_y'' , P_u'' :unstrengthened

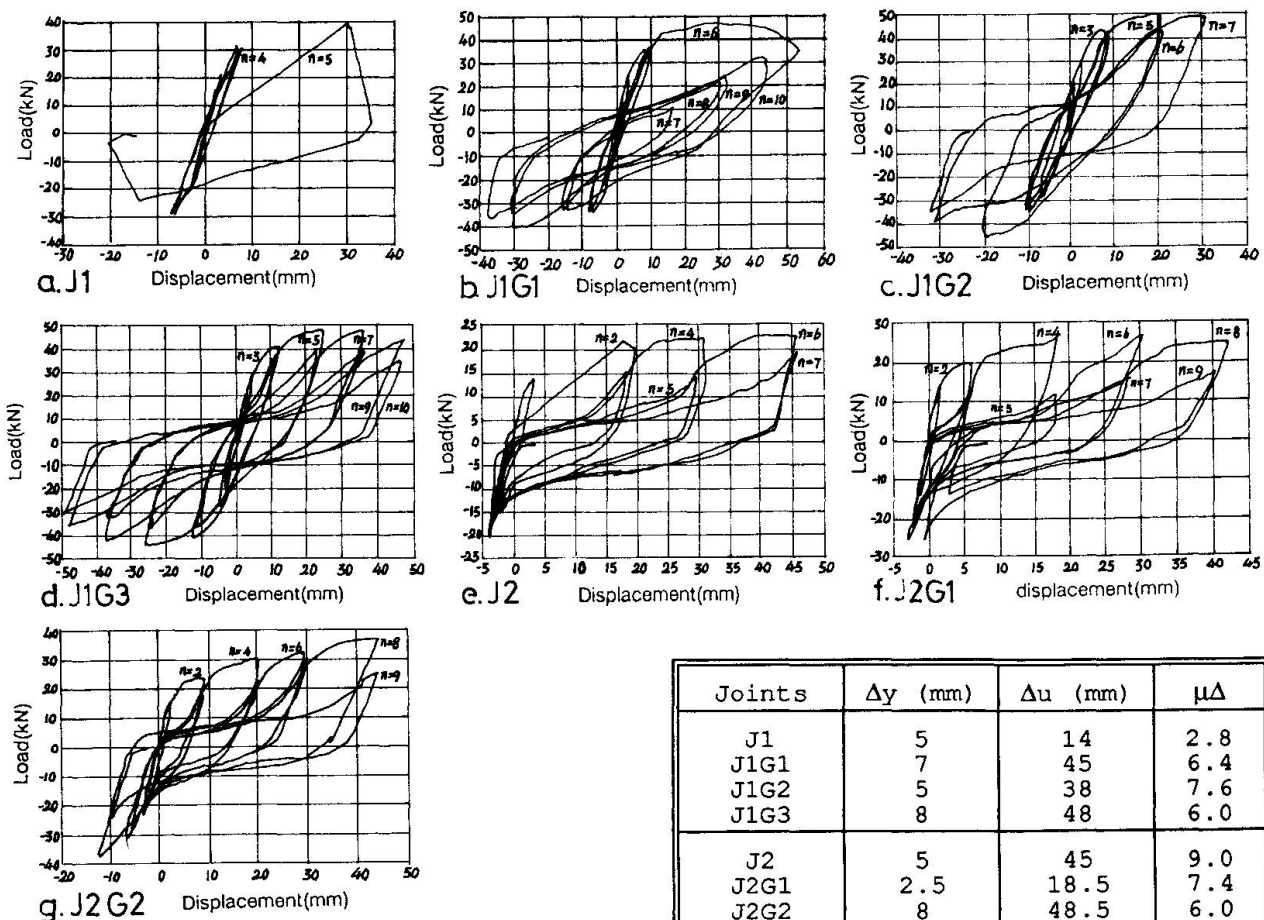
Table 2. Yield and ultimate loads

3. EXPERIMENTAL RESULTS

3.1 General description

The forms after the specimens collapsed are shown in Fig.3. In SET I, abrupt shearing failure took place at the core of J1, where the cracks were wide and long, and some concrete was peeled off. The plastic hinge in J1G1, however, was presented at the column section while only some small horizontal cracks developed at the core, which means the shearing strength at the core had been greatly enhanced. In J1G2, because of the strengthening by the angle steel at the column corners, the shearing strength at the core and the flexural compressive strength of the column had been greatly improved, thus, the plastic hinge occurred at one of the beam ends although many shearing cracks also developed at the core as shown in Fig 3.c. Fig 3.d presents the failure of J1G3 in which two obvious diagonal cracks were developed to indicate the shearing failure at the core contrasting with the plastic hinge at the beam end in J1G2.

In SET II, plastic hinges developed at the beam ends in each specimen as shown in Fig.3. In J2, the displacement in positive direction was very large when its load was small because of the very small positive flexural strength at the beam ends. J2G1 had exhibited almost the same behavior of deformation as that of J2 though it had been strengthened with the glued steel plates. This is because that the anchorage between the steel plates and the column failed after the second cycle of loading, and thus the steel plates could bear little tensile stress. In J2G2, however, it was different from J2G1 in that J2G1 did not have a continuous steel plate across its column. The steel plates of J2G2 could bear both tensile and compressive stresses since they were placed continually by being glued on the lateral surfaces of the beam, and its bearing capacity was much larger than that of J2 or J2G1 though it also developed plastic hinges at the beam ends just as J2 and J2G1 did.



Joints	Δy (mm)	Δu (mm)	$\mu \Delta$
J1	5	14	2.8
J1G1	7	45	6.4
J1G2	5	38	7.6
J1G3	8	48	6.0
J2	5	45	9.0
J2G1	2.5	18.5	7.4
J2G2	8	48.5	6.0

Fig.4. Load-displacement curves

Table 3. Displacement Coefficients of Ductility



3.2 Bearing capacity under seismic loads

The yield loads and the ultimate loads of different specimens are given in Table 2. The ratios of the loads after being strengthened to those before being strengthened are also presented in Table 2. All the strengthening methods in SET I had greatly improved the shearing strength at the cores, and both the yield and the ultimate loads were increased remarkably compared with those of J1. In SET II, however, only J2G2 had greatly improved the flexural strength of the beam ends while J2G1 almost remained unchanged because of the anchorage failure between the glued steel plates and the column.

3.3 Load-displacement curves

From the recorded data of the loads and their relative displacements at the free ends of the beams, the load-displacement curves of each specimen can be graphed as presented in Fig.4. As $\mu\Delta = \Delta_u / \Delta_y$ where $\mu\Delta$ is the displacement coefficient of ductility, Δ_u is the ultimate displacement and Δ_y is the displacement when the beam-column joints yielded, it is possible to calculate the $\mu\Delta$ values. These values are presented in Table 3. From the curves shown in Fig.4 and the values of $\mu\Delta$ in Table 3, it is very clear that the seismic behavior in SET I had been greatly improved after the joints had been strengthened, because the shearing strength and deformation capability had been increased remarkably and their displacement coefficients of ductility were also much larger than that of J1. In J1G1, since the displacement in the positive direction in the sixth cycle went so far away from the control that much more plastic deformation had developed in this direction than expected, consequently the peaks in this direction of the following cycles of loading were much lower than that of the sixth cycle. It may be supposed that the curves in this positive direction would have been more reasonable if there were not so much displacement in the sixth cycle. In SET II, the curves in J2G2 are much more precipitous than those of J2, and the flexural strength developed was much larger than that of J2, which means that this strengthening method can not only increase the carrying capacity but the flexural rigidity as well. However, it still had a reasonable value for the displacement coefficient of ductility needed for the beam to develop suitable deformation. As to J2G1, it is necessary to improve this kind of strengthening method.

4. CONCLUSIONS

These trial experiments have successfully made comparison between different strengthening methods with externally glued steel to improve both the shearing strength of the cores and the flexural strength at the beam ends. In SET I, all three strengthening methods can greatly improve the seismic behavior of the cores, although J1G2 presented a more reasonable failure mechanism than that of J1G1 or J1G3. However, J1G2 needs more complex construction than those of the latter. When the methods of J1G1 or J1G3 are adopted, suitable adjustment is needed to avoid abrupt failure such as the compressive yield at the column sections or the shearing failure at the cores.

In SET II, the strengthening method of J1G2 can greatly increase the flexural strength of the beam ends, while the method of J2G1 was a failure, and requires further improvement.

5. ACKNOWLEDGEMENT

Special thanks are due to Professor Jiang Dahua, for his invaluable assistance to this experimental program. The strengthening construction of the specimens was completed by the Shanghai Huili Project Contracting Department. This support is gratefully acknowledged. The writer also acknowledges the assistance of Mr. Ren Yuhe, who was a former graduate student at Tongji University.

REFERENCE

1. SHENTU L., Cyclic Behavior of Concrete Beams Strengthened with Glued Steel Plates, Journal of Structural Engineer (in Chinese), No.4, 1993.

Behavior of Precast Wall Connections for Strengthening Reinforced Concrete Frames

Comportement d'assemblages de panneaux préfabriqués
pour renforcer des cadres en béton armé

Verhalten vorgefertigter Wandverbindungen
zur Verstärkung von Stahlbetonrahmen

Wanzhi LI

Graduate Assistant
University of Texas at Austin
Texas, TX, USA

Robert J. FROSCH

Graduate Assistant
University of Texas at Austin
Texas, TX, USA

James O. JIRSA

Professor
University of Texas at Austin
Texas, TX, USA

Michael E. KREGER

Associate Professor
University of Texas at Austin
Texas, TX, USA

SUMMARY

A novel technique using precast concrete panels to strengthen or repair non-ductile reinforced concrete frames is presented. Tests of panel-to-panel and panel-to-frame connections are discussed. In particular, shear key geometry and arrangement, closure strip height and reinforcement, and panel and closure strip concrete strengths are examined for the panel-to-panel connections. Embedment depth of shear lugs in the frame segment and closure strip is studied for the panel-to-frame connections. The impact of the test variables on specimen ultimate strength and residual shear strength is examined.

RÉSUMÉ

L'article traite d'un nouveau procédé pour renforcer ou réparer des cadres en béton armé peu ductiles, au moyen de panneaux en béton préfabriqués. Les auteurs examinent les assemblages des panneaux entre eux et ceux des panneaux aux cadres. Dans le cas du premier type de liaison, ils soulignent l'importance de la forme géométrique et de la disposition des clavettes de cisaillement, l'épaisseur et l'armature des bandes de béton coulé sur place, ainsi que le rapport de la résistance du béton coulé sur place à celle du panneau préfabriqué. Pour le deuxième type de liaison, il y est question de la profondeur d'encastrement des raccords de cisaillement dans les cadres et dans les bandes de béton coulé sur place. Les auteurs soulignent l'influence des paramètres d'essais sur la résistance ultime et la résistance résiduelle au cisaillement des échantillons.

ZUSAMMENFASSUNG

Es wird ein neuartiges Verfahren zur Verstärkung oder Reparatur wenig duktiler Stahlbetonrahmen mittels Fertigteilscheiben vorgestellt. Dabei werden die Verbindungen der Scheiben untereinander und zum Rahmen angesprochen. Für erstere werden die Formgebung und Anordnung von Schubnocken, die Dicke und die Bewehrung des Ortbetonstreifens und das Verhältnis der Ortbetonfestigkeit zur Fertigteilfestigkeit erörtert; bei der Verbindung zwischen Scheibe und Rahmen werden die Einbindetiefe von Schubanschlüssen im Rahmen und im Ortbetonstreifen untersucht. Der Einfluss der Testparameter auf die Traglast und die Restschubtragfähigkeit der Prüfkörper wird gezeigt.



1. INTRODUCTION

The use of precast concrete infill walls and post tensioned boundary members to strengthen and repair nonductile reinforcement concrete frame structures is a technique that takes advantage of the shear capacity of infill walls and moment capacity afforded by post-tensioning tendons adjacent to the boundary columns. The objective of this study is to develop a viable repair and strengthening technique that will greatly reduce construction time and cost.

The infill wall consists of several precast concrete panels united by closure strips. The panels will be connected to the existing frame elements using special shear dowels or lugs located in the boundary closure strips [Fig. 1]. Post-tensioned tendons adjacent to the existing columns will supplement the tensile capacity of the existing columns and delay opening of the horizontal closure strips.

To investigate the behavior of panel-to-panel and panel-to-frame connections, fifteen specimens were constructed and tested. The specimens were subjected to reversed cyclic loads which were initially applied in a load-control mode. When the specimen had softened considerably, displacement control was used. All joint specimens were tested using the setup shown in Fig. 2. The remainder of this paper focuses on the connection test program and results.

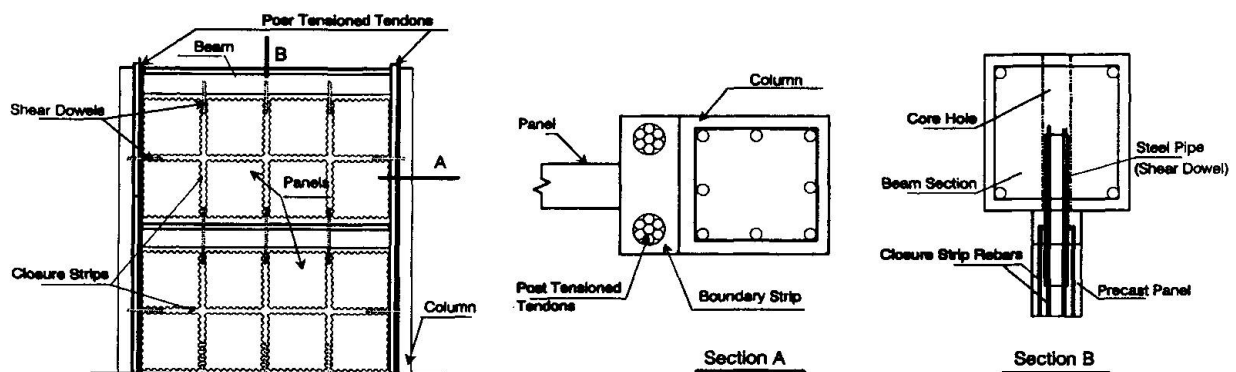


Fig.1 Precast Infill Wall System

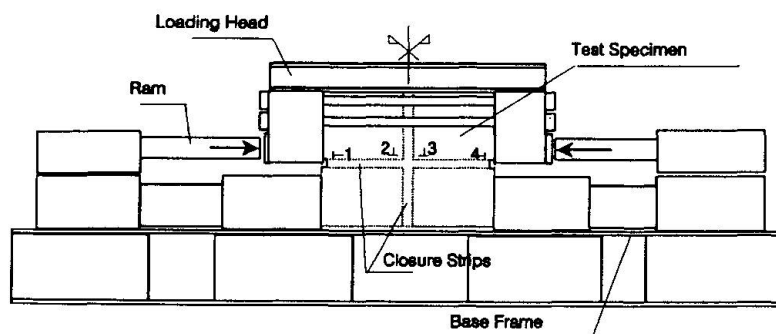


Fig. 2 Connection Specimen Test Set-Up

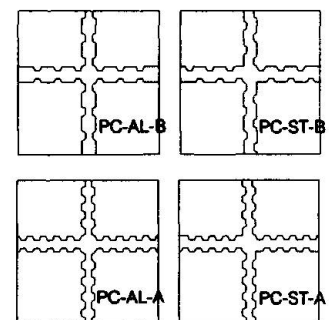


Fig. 3 Panel Connection - Key Patterns

2. PANEL TO PANEL CONNECTIONS

The weight and dimensions of precast panels will be limited to allow transport of the precast panels inside the building using a compact forklift during construction. The panel dimensions will be a function of the limiting weight, dimensions of the frame to be retrofitted and wall thickness. For example, a panel weighing approximately 8000 to 9000 kN with thickness of 15 cm would be as large as 150x150 cm. Twelve panel to panel connection specimens with thickness of 15 cm and dimension of 125x90 cm were tested in the studies. Key patterns, closure strip dimensions and reinforcement and comparable strength of the panels and grout material in the closure strips were variables in the studies.

2.1 Key Patterns

In order to allow shear transfer between panels, panel edges were cast with shear keys. Four specimens were cast initially with different key patterns as illustrated in Fig. 3. The specimens were full-scale representations of the connections located at the intersection of four panels. The panels were constructed with 35 MPa concrete and the closure strips were grouted with 50 MPa concrete containing 1.0 cm aggregate. Casting of joints was conducted with the panels in the vertical position to simulate the casting process that would be used in the field. The shear keys were 2.5 cm high and were positioned so the length of the crests and troughs were the same. For the less dense pattern, the length of the trough was increased by 50%. Keys on opposite sides of the closure strip were positioned to be aligned or staggered. The clear height of the closure strip was 5 cm and two #3 (0.95 cm diameter) rebars were placed in both the horizontal and vertical closure strips.

The tests were conducted under direct shear along the horizontal closure strip. No other loads were applied to the specimens. The observed responses for the four specimens were quite similar. An example of measured load-interface slip response for specimen PC-1 (PC-AL-A) is illustrated in Fig. 4. It was noted that:

- (1) The failure was typically the result of a direct shear failure through the base of the panel keys. In this test, the panel concrete strength was much lower than the closure strip concrete strength.
- (2) The residual strength or shear friction strength of the specimens was substantially lower than the peak strength of the uncracked specimens. In fact, the rebars in the vertical strip yielded [Fig. 5] completely and the residual strength was primarily dependent on the ultimate strength of the vertical closure strip rebars.
- (3) Both aligned and staggered key patterns gave approximately the same shear capacity for the same key geometry.
- (4) Some air was trapped between the precast panels and the top of the closure strip concrete. There was lack of adhesion at the interface.

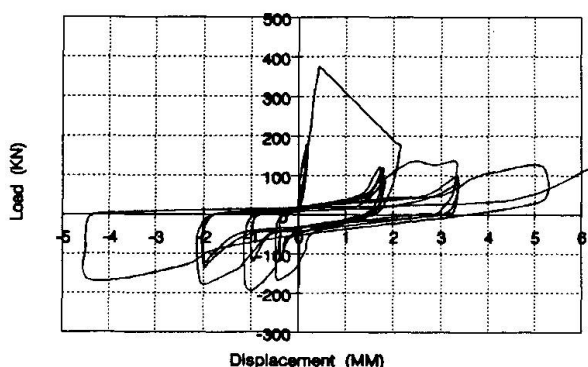


Fig. 4 Load-Interface Slip of PC-1

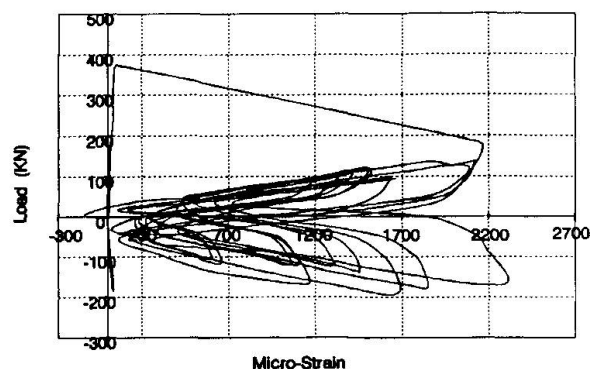


Fig. 5 Load-Rebar Micro Strain of PC-1



2.2 Strip Height

Although smaller closure strip heights result in placement of a small volume of concrete grout needed to construct the infill wall, they also make grouting of the closure strip difficult. It was not possible to grout the horizontal closure strip by placing grout from the vertical strip when the horizontal strip had a clear height of 5 cm. Furthermore, placing more rebars in the vertical closure strip to increase shear friction or placing shear lugs (described later) between the infill wall and existing frame requires a larger closure strip.

Several specimens were built with a clear closure strip height of 10 cm. The panel concrete strength was 30 MPa and the grout strength was 48 MPa. Specimen PC-5 was reinforced with 2-#3 rebars. Its ultimate strength was 310 KN and residual strength was 120 KN. Compared with the results of specimen PC-1 [Table 1], which had an ultimate strength of 374 KN, the lower strength of PC-5 was apparently the result of lower panel concrete strength. This suggests the ultimate direct shear strength is proportional to the panel concrete strength when the grout strength is higher than the panel concrete strength.

Although the closure strip height did not apparently affect the ultimate strength of the specimens, a 10 cm strip provided better conditions for grouting. By adding superplasticizers to increase the grout slump to 20 cm or more, it was possible to cast the horizontal closure strips by placing grout through the vertical closure strip if some small openings were left in horizontal closure strip. The small openings provided in the horizontal closure strip focus to release entrapped air. The closure strip casting quality was much better than that of the 5 cm strip. In addition, the 10 cm strip was suitable for four or more rebars and the shear lugs that will be placed later.

2.3 Reinforcement

As mentioned previously, the reinforcement in the vertical closure strips played an important role in the shear friction strength. Within a certain range, more vertical strip reinforcement results in higher shear friction strength. Fig. 6 illustrates the load-interface slip response of specimen PC-8. Comparing specimens PC-5 and PC-8, the vertical closure strip rebars increased from 2-#3 to 4-#4 (1.27 cm diameter bars) while the shear friction strength increased from 120 KN to 267 KN.

According to the test results and analysis, the shear friction is related to specimen ultimate strength, specimen cross section and vertical closure strip reinforcement. The ultimate strength also appears to be related to the amount of vertical closure strip reinforcement. Comparing PC-5 with PC-9 and PC-10 [Table 1], the ultimate strength for the latter two was 50% higher than the strength of the former because of the increase in the vertical closure strip steel.

When the vertical steel exceeded a certain level, the specimen experienced a concrete failure demonstrated by specimen PC-12. There were 6-#5 (1.59 cm diameter bars) rebars in the vertical strip and the ultimate load applied was 900 KN.

2.4 Grout Strength

All specimens except PC-7 were grouted with concrete having a strength of between 40 MPa and 50 MPa while the panel concrete strengths were between 30 and 35 MPa. Because the grout strength was between 1.4 and 1.6 times the panel concrete strength, the failure of the specimens was typically along the base surface of the panel keys. In order to investigate the effect of grout having a lower compressive strength than the panel concrete, specimen PC-7 was grouted with concrete having 22 MPa concrete strength. Failure of this specimen was along the base surface of the closure strip keys.

2.5 Influence of Loading

All the specimens discussed to this point were tested under direct shear. This type of direct shear load between panels will obviously not exist in actual precast infill walls. Nonetheless, it was used to identify the best details for joining together precast infill panels. In order to simulate a more realistic loading mode on these connections, a compressive load was applied vertically on the specimen by tightening the loading head down to the base. Unlike the connections tested in direct shear which failed along the base of the panel or closure strip keys, connections subjected to combined load of direct shear and normal load experienced several diagonal cracks in the horizontal closure strip region. This type of cracking may be more representative of the behavior that will be experienced by actual panel-to-panel connections. Furthermore, the addition of vertical load also enhanced the ultimate strength.

It should be noted that this failure mode is based not only on the vertical load applied but also depends on the presence of a sufficient number of rebars in the vertical closure strip to prohibit premature failure of panel keys.

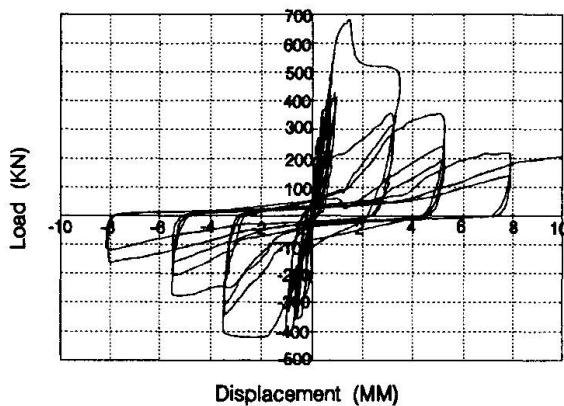


Fig. 6 Load-Interface Slip of PC-8

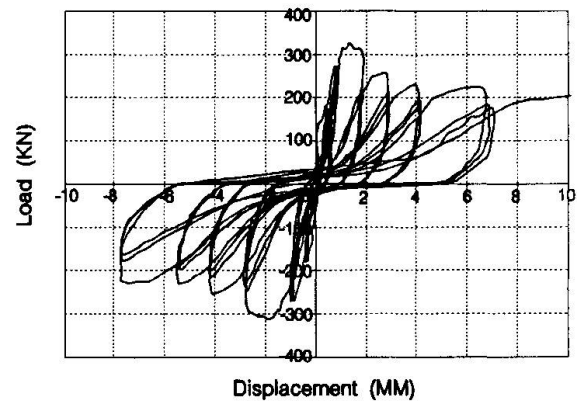


Fig. 7 Load-Interface Slip of FC-3

3. PANEL TO FRAME CONNECTIONS

In order to facilitate shear transfer along the interface between the precast infill wall and existing frame, a special shear dowel or lug made of a steel pipe will be embedded in the interface [Fig. 1]. In the infill wall, the closure strips provide space for the embedment of the shear dowels. For the existing frame, cored holes in beams and columns are used to embed the shear dowels.

3.1 Connection Specimen

The holes to be cored in beams have three functions: to permit the shear dowel embedment, to anchor vertical closure strip reinforcement, and to facilitate placement of closure strip concrete placing. The size of the hole should be determined based on the width of the beam, the size of the dowel pipe and the number of reinforced vertical closure strip bars. A 10 cm diameter hole was cored in a 45 cm wide concrete beam segment and a steel pipe with 7.5 cm outside diameter was embedded in the hole. Before embedding the pipe in the interface of beam



segment and precast panels, concrete was cast through the cored hole into the closure strips. Three specimens with various combination of pipe embedment in the closure strip and beam segment were cast and tested.

Table 1 Test Specimen Properties

member	f_c of panel	panel thickn.	key height	key space	strip height	f_c of strip	rebars	peak load	residual strength	Load condn.	remark
PC-1	35.5 MPa	15 cm	2.5 cm	6.25 cm	5 cm	50.1 MPa	2-#3	374 KN	—		PC-ALA
PC-2	35.5	15	2.5	9.375	5	50	2-#3	276	—		PC-ALB
PC-3	35.5	15	2.5	6.25	5	50	2-#3	325	—		PC-STA
PC-4	35.5	15	2.5	9.375	5	50	2-#3	310	—		PC-STB
PC-5	29.7 MPa	15	2.5	6.25	10	47.7	2-#3	310	120 KN		Aligned
PC-6	29.7	15	2.5	6.25	10	47.7	4-#4	797	—	Vert. L	Aligned
PC-7	29.7	15	2.5	6.25	10	22.2	4-#4	455	262		aligned
PC-8	29.7	15	3.75 cm	9.375	10	47.7	4-#4	680	267		Aligned
PC-9	29.7	15	2.5	6.25	10	47.7	4-#3	460	178		Aligned
PC-10	29.7	15	2.5	6.25	10	47.7	2-#4	484	178		Aligned
PC-11	29.7	15	3.75 cm	9.375	10	47.7	4-#3	697	205	Vert. L	Aligned
PC-12	29.7	15	2.5	6.25	10	47.7	6-#5	900	—	Vert. L	Aligned
FC-1	29.7	15	2.5	6.25	10	47.7	23/10*	283	—		Aligned
FC-2	29.7	15	2.5	6.25	10	47.7	23/23	315	205		Aligned
FC-3	29.7	15	2.5	6.25	10	47.7	10/23	327	209		Aligned

* where 23/10 means the pipe embedded 23 cm and 10 cm in frame and panel respectively

3.2 Shear Dowel Performance

Because there were no shear keys in frame member segment, the interface between the retrofit element and frame member segment cracked at lower load than the panel-to-panel connection specimens. As a result, the steel pipe began resisting shear at a relatively low load. Under cyclic load, the concrete developed a bearing failure on each side of the pipe and the pipe yielded. A conclusion of the tests, the panels were split along their axes.

The different pipe embedments resulted in no significant differences in measured ultimate strengths. However, it is necessary to embed the pipe in closure strip with sufficient length to fully develop its yield. Specimen FC-1 with 10 cm pipe embedment in the closure strip developed slightly lower ultimate strength and could not develop significant residual shear strength before failing. Both FC-2 and FC-3 with a pipe embedment of 23 cm in the closure strip developed significant higher ultimate strength and significant residual strength [Fig. 7]. The residual strength of panel-frame connection is approximately the shear yield strength of the steel pipe.

4. CONCLUSIONS

A novel technique utilizing precast infill wall panel to strengthening or repair non-ductile reinforced concrete frames was presented. Results of cyclic load tests on panel-to-panel and panel-to-frame connections were discussed. The factors influence the performance of panel to panel connection were the height of the closure strips, the quantity of vertical closure strip reinforcement and the type of load mode. For a limited number of panel-to-frame connections, the size and embedment of the shear dowel were believed to have significant affect on the connection ultimate and residual strengths. To investigate the behavior of these connection details worked with post tension in a precast infill wall system under more complex loads, a large scale test frame is currently being constructed and will be tested.

Seismic Performance of Older Steel Frames
Comportement parasismique de vieux cadres métalliques
Seismisches Verhalten von älteren Stahlfachwerken

Roberto T. LEON

Professor
Georgia Institute of Technology
Atlanta, GA, USA

Gabriel P. FORCIER

Post-Doctoral Fellow
University of Minnesota
Minneapolis, MN, USA

Charles W. ROEDER

Professor
University of Washington
Seattle, WA, USA

F. Robert PREECE

President
Preece, Goudie & Assoc.
San Francisco, CA, USA

SUMMARY

To study the performance of older steel frames, over twenty bolted and riveted connection specimens were tested and companion analytical studies conducted. The experimental results indicate that the cyclic performance of riveted connections governed by rivet shear capacity is poor, and that their hysteretic behavior degrades rapidly. The effect of encasement is to considerably strengthen and stiffen the frame and delay the degradation.

RÉSUMÉ

Dans le but d'étudier la performance de cadres métalliques anciens, plus de vingt spécimens furent testés. Cette étude fut complétée par des calculs numériques. Les résultats expérimentaux indiquent que les réponses cycliques des connexions dont les déformations majeures proviennent du cisaillement des rivets, et ont des boucles d'hystérèse se dégradant rapidement. Les effets des revêtements en béton permettent d'augmenter considérablement la rigidité et la résistance des cadres ainsi que de retarder leur dégradation.

ZUSAMMENFASSUNG

Zu der Untersuchung der Leistung von älteren Stahlfachwerken wurden über zwanzig Versuche an geschraubten und genieteten Verbindungen im vollen und im Dreiviertel-Massstab gemacht, mit gleichzeitigen rechnerischen Studien. Die Versuche zeigten, dass die zyklische Leistung der genieteten Verbindungen, wenn die Stärke von der Schraubkraft der Nieten bestimmt ist, mangelhaft ist und dass ihr hysteritisches Verhalten schnell degradiert. Die Wirkung der Umhüllung ist eine erhebliche Verstärkung und Verstiftung des Fachwerkes und eine Verschiebung der Degradation.



1. Introduction

The recent 1994 Northridge and 1995 Kobe earthquakes have once again emphasized the need to develop accurate techniques to evaluate the seismic safety of older structures. Among the classes of structures that have traditionally performed very well in moderate and large earthquakes is the older steel moment resisting frames. These structures, dating from the first half of this century, are substantially different from steel moment frames erected more recently. The main differences are in the detailing of the connections, the encasement of the beams and columns, and the presence of heavy infill walls typical in this type of older construction. While designed as moment frames, these buildings probably would not respond as such under large seismic loading. Because of the infills these buildings will probably behave as stiff masonry structures initially, with their behavior shifting to that of steel frames as the infills failed. The effect of the encasement will probably remain for much larger deflections than that of the infills, but the degree of composite action is uncertain. These structures are potentially brittle because the larger forces resulting from the added mass of the encasement and infill walls cannot generally be accommodated by the frame alone unless substantial connection ductility and energy dissipation can be provided. In this regard the main concern is the cyclic performance of steel connections fabricated with rivets, since little experimental data was available to generate models or provide guidance in an evaluation process. This paper reports on the results of an analytical and experimental study aimed at determining the performance of the connections in older steel frames, with emphasis on the effects of the rivets and the encasement. The main aim of the research was to assess the strength, stiffness and ductility of these steel frames.

2. Background

Older steel frames (prior to about 1950) were erected utilizing complex riveted connections and members. The main members were routinely encased in concrete or masonry for fire-proofing. The encasement was often cast integrally with the floor slabs which contained appreciable amounts of mild, undeformed steel reinforcement. The dimensions and quality of the encasement varied widely, but it is well known that some degree of composite action will be activated in such members even if shear connectors are not present. The net result is that these frames cannot be evaluated as pure steel moment frames since this would overestimate the natural period and reduce the design forces in the structure. The evaluation of these buildings is complicated by the fact that these buildings were designed for relatively low equivalent lateral loads and do not comply with current seismic design provisions. Strengthening and retrofitting of these frames would probably be prohibitively expensive and technically unjustifiable given that a large number of these buildings have performed very well in past earthquakes (1906 San Francisco and 1923 Great Kanto events, for example).

To study the performance of these older steel frames, a joint experimental and analytical study was undertaken by the U. of Washington, the U. of Minnesota, and Preece, Goudie and Assoc. The study was divided into experimental and analytical tasks. The experimental part was aimed at determining the cyclic behavior of a wide class of riveted connections. This knowledge was then utilized in the analytical

studies to develop and study both local models for the connection response and global models for use in frame analysis.

3. Experimental Study

Data on the behavior of full-sized riveted connections subjected to large load reversals is scant. With the exception of several tensile tests carried out in the wake of the Quebec Bridge disaster [1] and a single bending test in the 1930's [2], little or no cyclic studies on riveted connections are documented in the literature. To obviate the need for more experimental data, seven full-scale and sixteen 3/4-scale specimens were tested in this program. The connections tested included T-stub, top-and-seat angle, and stiffened seat connections, with and without encasement, and utilizing a variety of connector (rivets, modern high strength bolts, and high strength friction bolts.) The specimen configuration was taken directly from the connections in a 26-story frame erected in San Francisco in 1926. This building was deemed to be typical of the construction of that period and had already been evaluated by Preece, Goudie, and Assoc.

Due to space limitations only the results of selected full-scale specimens tested at the U. of Minnesota will be discussed here. Details of the complete test series are available elsewhere [3]. Cruciform specimens, about 4 m high by 6 m long, utilizing both stiffened seat and T-stub connections were used. They were loaded by displacing the bottom of the column under a slowly increasing pattern of alternating loads to simulate the seismic forces. The only important departure in these specimens from the prototype building was in the column size. This was reduced since no meaningful axial loads could be applied to such large specimens and the effect of axial load on connection behavior was assumed to be small. The specimen discussed here all utilized the T-stub connection shown in Figure 1.

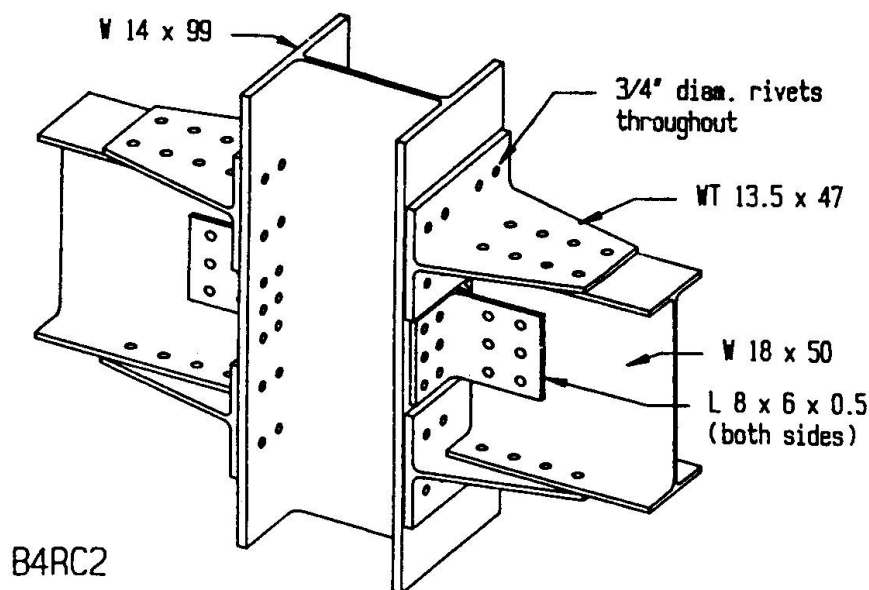


Figure 1 - Typical riveted connections used in the tests.



One of the more important features of these tests is the use of 19 mm A502 Grade 1 rivets ($F_y = 310$ MPa, $F_u = 413$ MPa), very similar to those used in the real structure. For these tests standard size holes, about 1.6 mm larger than the rivet diameter, were used for the connection. The rivets were heated to at least 1000 C and then shaped with pneumatic hammers. The riveted connections were fabricated following typical practice as verified by several experienced riveters. Post-test sections cut across the connections showed that the holes were properly filled by the rivets.

The first three tests were run on all-steel specimens, with the only variable being the connector type: rivets (A502 Grade 1), black bolts (A307), and friction bolts (A325). Figure 2 illustrates the moment-rotation behavior of these specimens. The pronounced pinching behavior in the riveted specimen was surprising and contrary to what many researchers had assumed in the past. The pinching was due primarily to slip at the shear interface where very large local deformations had taken place. This in turn led to an elongation of the rivet and a rapid loss of any clamping action. The energy dissipation capacity decreased rapidly with increasing deformations, but the connection regained stiffness and strength once the rivets went into bearing. Typically these hysteresis loops would be considered unsatisfactory. However, the load history imposed was severe and in the real structure the connection would have benefited from additional restraints and force redistribution. Thus the performance of a structure incorporating these connections would probably be better than gleaned from this isolated example.

In the remaining tests, which included the effect of encasement and floor slabs, the behavior improved markedly. The encasement increased both the strength and stiffness of the specimens even though there were no shear studs in the beam or column. In fact, the measured response indicated that the sections behaved as fully composite under cyclic loads until the cover concrete began to crush around drifts of 2.5%. The beneficial effect of the concrete cover was also surprising since the confinement steel was minimal. The concrete also acted to restrain the slip. Although a crack formed at the beam-column interface early in the load history, it did not grow appreciably resulting in smaller rotations for the encased specimens than for the all-steel specimens. Two mechanisms can be postulated to explain this behavior. First, in the compression side of the connection the concrete transferred most of the force directly by bearing directly into the end of the T-stub and the column directly. Thus no appreciable shears were induced in the rivets and the resulting slip was very small. Second, in the tension side of the connection the rivet heads provided an additional load transfer mechanism by bearing, which in addition to the friction between the two materials, resulted in only the first few rivets being loaded to their yield in shear. As the loading progressed the web of the T-stub began to yield resulting in a stable hysteretic response. Connections governed by yielding in the beams or connecting plates, which were tested as part of this program, performed better but at large deformations loss of cover resulted in large strength losses [3].

4. Analytical Studies

Two general approaches, a local and a global one, were used to model the connections. The intent of the former was to develop comprehensive local models

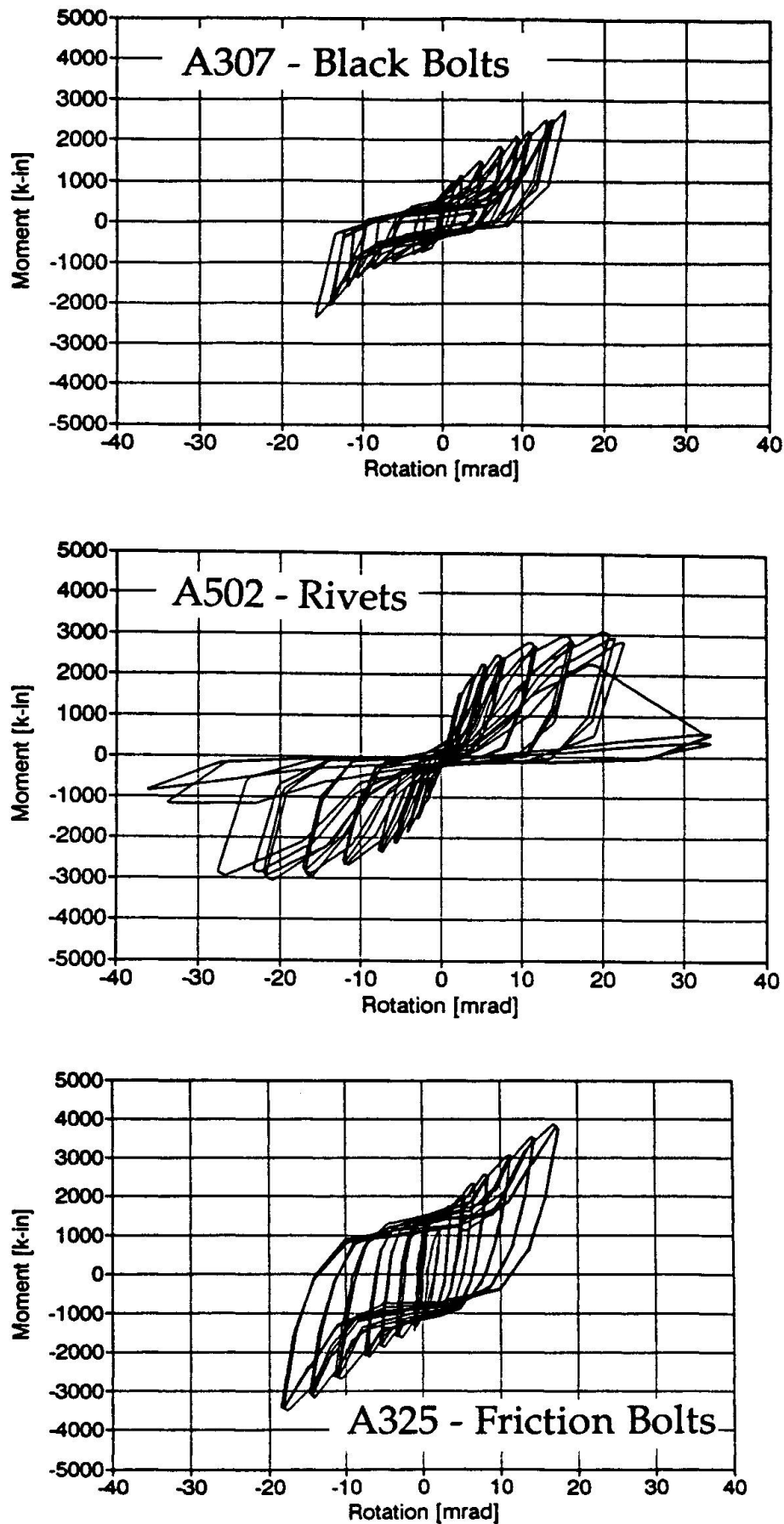


Figure 2 - Comparison of moment-rotation behavior.



utilizing finite elements. For the case of the all-steel connections a new element to describe the local shear behavior was developed utilizing ABAQUS. This element was successful at modeling the degrading behavior shown in Fig. 2. Theoretically this approach is very accurate, but the numerical difficulties encountered while trying to model the conditions at the interfaces of the assemblages render it very difficult for cases with several large load reversals[3]. This is particularly true when the composite action and slip need to be included simultaneously.

The second approach is of a more macroscopic nature. This second method consists of modeling the subassemblages with large structural elements, where different minute connection effects (slip, yielding and friction) are lumped together into dimensionless rotational springs at the beam ends. The panel zone area is modeled with a planar element allowing for shear deformation only. Non-linearities are handled by relationships between the forces applied on the elements and their associated deformations. These relationships can be derived from experiments, or from any other suitable method. Use of this latter method leads to a problem of much smaller size. Studies of small frames (up to 10 stories) utilizing these models indicated that the frames possessed the necessary strength and ductility to survive ground motions of up to 0.4g.

5. Summary

The experimental results indicate that the cyclic performance of riveted connections governed by rivet shear capacity is poor, and that their hysteretic behavior degrades rapidly. The effect of the encasement is to considerably strengthen and stiffen the frame and delay the degradation. The companion analytical studies centered on non-linear dynamic analysis of 8 to 10 story frames indicate, however, that the performance of the frames will be acceptable if an accurate modeling of the connection behavior, including slip and panel zone yielding, is made.

6. Acknowledgements

This work was sponsored by the National Science Foundation under the Repair and Rehabilitation Research Project (R/R).

7. References

1. GOVERNMENT BOARD OF ENGINEERS, The Quebec Bridge. Vol. 1, Department of Railways and Canals, Ottawa, 1919.
2. YOUNG C.R. and JACKSON K.B, The Relative Rigidity of Welded and Riveted Connections, Canadian Journal of Research, Vol. 11, No. 1, July 1934
3. ROEDER C.W., LEON R.T, and PREECE F.R., Strength, Stiffness, and Ductility of Older Steel Frames, Report No. SGEM 94-4, Department of Civil Engineering, The University of Washington, Seattle, WA, December 1994.

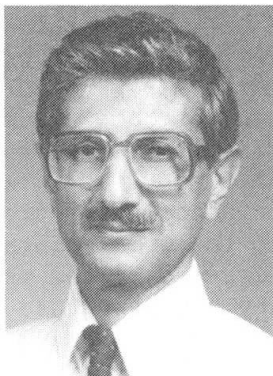
Reinforced Concrete Sheath for Repair of Damaged Masonry Walls

Enveloppes en béton armé pour renforcer les murs en maçonnerie endommagés

Stahlbetonmembranen zur Reparatur beschädigter Mauerwerkswände

Bezaleel BENJAMIN

Professor
University of Kansas
Lawrence, KS, USA



Bezaleel Benjamin, born in 1938, received his B.E.(Civil) from Bombay Univ. and has both M.Sc(Eng) and Ph.D. degrees from the University of London. He is now Professor of Architecture and Architectural Engineering at the University of Kansas, where he has taught for the past 24 years.

SUMMARY

This paper describes theoretical and experimental work on the use of a thin, reinforced concrete sheath for the repair of load-bearing masonry walls damaged by earthquakes. The thin sheath is prevented from buckling by the cracked masonry wall to which it is tied. The experimental work on model walls investigates the reserve strength, in buckling, of severely cracked masonry walls under vertical loading. It then determines the improvement in load-carrying capacity by the provision of the thin sheath tied to the old wall. The sheath can then be faced to return the building, visually, to its original architectural appearance.

RÉSUMÉ

Cet article décrit les travaux théoriques et expérimentaux destinés à la consolidation de murs porteurs en maçonnerie endommagés par les effets sismiques. Ce renforcement prévoit d'enrober les structures défailtantes par des voiles minces en béton armé, ancrés dans la maçonnerie fissurée de façon à en empêcher le flambement local. A partir d'études expérimentales sur modèles de parois, l'auteur examine la capacité portante résiduelle sous charge verticale des murs fortement fissurés, puis détermine la résistance complémentaire que doivent assurer les enveloppes de consolidation. Il indique en outre la possibilité de revêtir les voiles d'enrobage pour redonner aux bâtiments leur aspect architectural initial.

ZUSAMMENFASSUNG

Der Beitrag beschreibt theoretische und experimentelle Arbeiten zur Reparatur erdbebengeschädigter tragender Mauerwerkswände mittels dünner Stahlbetonumhüllung. Die dünnen Membranen werden durch Ankerung an das gerissene Mauerwerk am Ausbeulen gehindert. Die experimentelle Arbeit untersucht die Resttragfähigkeit der stark gerissenen Mauerwerkswände gegenüber Instabilität unter Vertikallast. Anschliessend wird die Erhöhung der Tragfähigkeit infolge der hinzugefügten Membranen bestimmt. Die Membran kann zusätzlich verkleidet werden, um dem Gebäude optisch sein ursprüngliches architektonisches Aussehen zurückzugeben.



1. INTRODUCTION

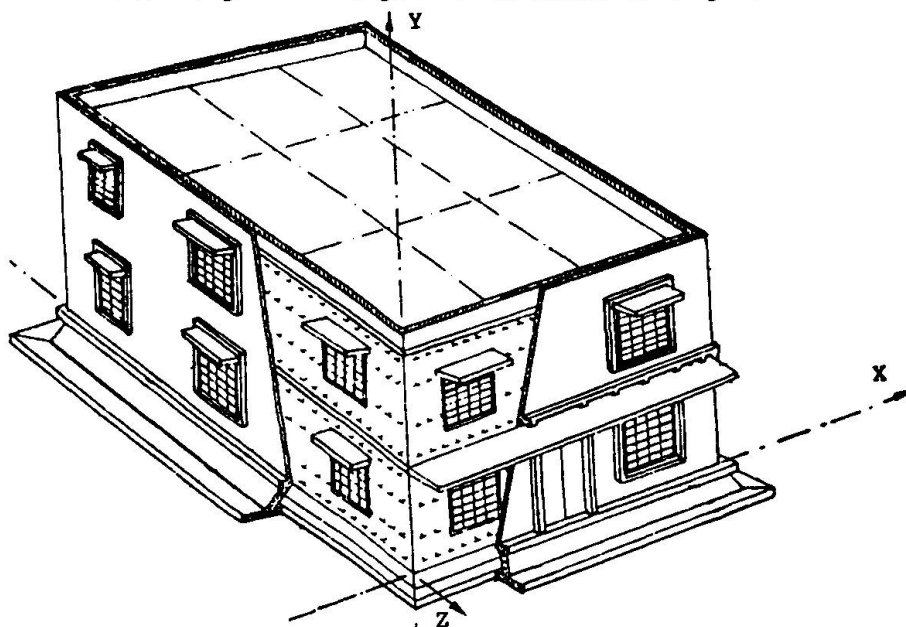
Load-bearing masonry walls damaged by earthquakes develop cracks that make the structure unusable. Existing Codes of Practice consider such walls to be unsafe, resulting in either the building being condemned or expensive renovation that often destroys the architecture of the building. Furthermore, in the case of historic buildings, damaged by earthquakes, both of the existing approaches would be unacceptable.

In all such cases, the assumption is made that cracked masonry walls do not have any reserve strength in buckling, to carry vertical loads, inspite of the fact that the building is still standing. A study of crack patterns shows that under horizontal loads, imposed by an earthquake, masonry walls develop shear failure with diagonal cracking. A photograph of the Oakland Hotel by Langenbach [1] shows this type of diagonal cracking in the external facade of the building. The cracks extend between spandrels at floor levels in the vertical direction and between window openings in the horizontal direction. The removal of internal partitions of that building, prior to the Loma Prieta earthquake of October 17, 1989, led to all the shear loads being carried by the external facade and may have contributed to the damage sustained by the structure [1].

2. THE REINFORCED CONCRETE SHEATH

2.1 The Author's Method

The author's method [2],[3] for the repair and strengthening of such buildings is to provide a thin, reinforced concrete sheath that is tied to the old, masonry wall structure. The thin sheath is prevented from buckling by the masonry wall behind it. The sheath passes around door and window openings and is strengthened by the provision of bands. The sheath was first proposed for load-bearing masonry structures in poor countries where changes in municipal regulations permitted vertical extension of old buildings by the addition of more stories than allowed for in the original design. It is shown in Fig. 1. While this paper considers



the reinforced concrete sheath tied to cracked masonry walls damaged by earthquakes, the theoretical analysis given here is still valid because it assumes that the sheath takes all of the vertical loads in the hybrid construction, provided it is prevented from buckling by the masonry wall behind it to which it is tied. Whether this assumption is valid or not has been determined experimentally in Chapters 3 and 4 of this paper.

Fig. 1 The reinforced concrete sheath

2.2 Theoretical Analysis of the Sheath

A theoretical analysis of the sheath [3] was carried out using the IMAGES-3D program under a vertical loading of 105 N/mm for seventeen different cases

involving variations in thickness of the sheath, size of bands around openings and base conditions. However, as the results showed, only cases A3, B3, D3, E3, F3, G3, with a 76 mm thickness of sheath, and O2 and P2, with a 51 mm thickness of sheath were acceptable, and these are shown in Table 1.

Case	Thickness	Openings	Band Size (mm)	Base	Notes
A3	76 mm	No	-----	Pinned	All plates in
B3	76 mm	No	-----	Fixed	All plates in
D3	76 mm	Yes	152 x 305	Fixed	Lintels and verticals
E3	76 mm	Yes	152 x 305	Pinned	Lintels and verticals
F3	76 mm	Yes	152 x 305	Pinned	All bands in
G3	76 mm	Yes	152 x 305	Fixed	All bands in
O2	51 mm	Yes	152 x 305	Pinned	All bands in
P2	51 mm	Yes	152 x 305	Fixed	All bands in

Table 1 Cases suitable for design and analysed by IMAGES-3D

The dimensions of the wall facades are shown in Fig. 2, with the lines relevant to the rest of the theoretical analysis. The absolute maximum stress in the wall plates and the deflection at Pt. 52, shown in Fig. 2, are given in Table 2 as follows.

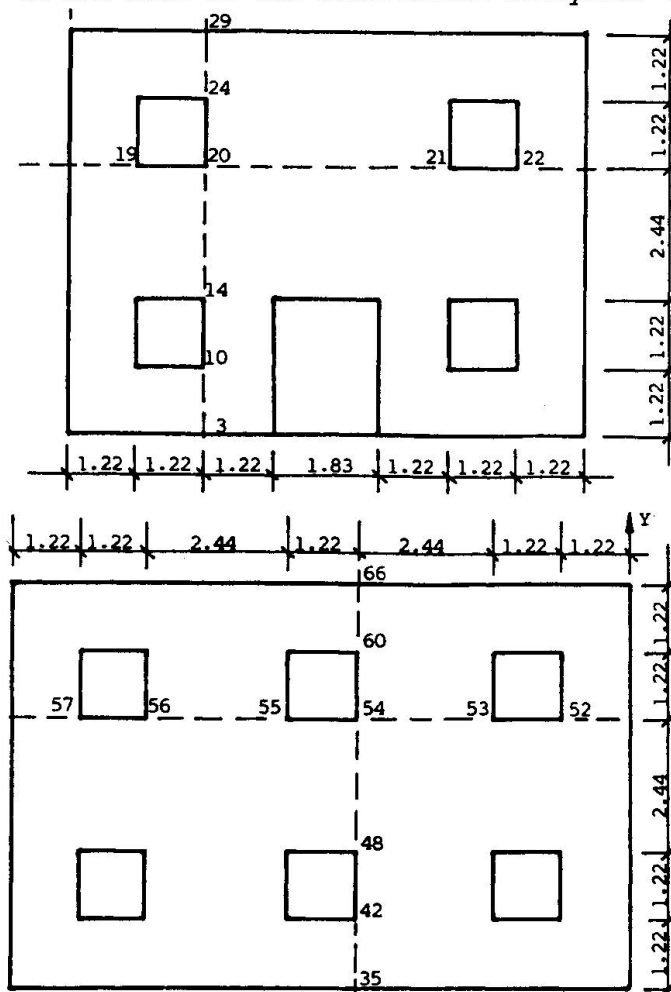


Fig. 2 Wall facades of the sheath

Case	Stress (N/sq mm)	Defl. mm
A3	2.854	1.18
B3	2.868	1.04
D3	3.013	0.86
E3	2.985	0.94
F3	2.758	0.97
G3	2.765	0.89
O2	4.357	0.99
P2	4.351	0.91

Table 2 Maximum stress in plates and deflection at Point 52

The horizontal deflections of the sheath for all of the cases analysed are shown along lines 19-22 and 52-57 in Fig. 3. A study of these deflections shows that the deflections of the unpunctured sheath (A3, B3) are small. Deleting the plates for door and window openings increased the deflections considerably. The insertion of sizeable bands, 152 mm x 305 mm around openings, however, returned



the sheath to a virtually unpunctured condition (D3, E3, F3, G3, O2, P2). Maximum deflections do not occur at the centre of the walls because of wrinkling in the plates.

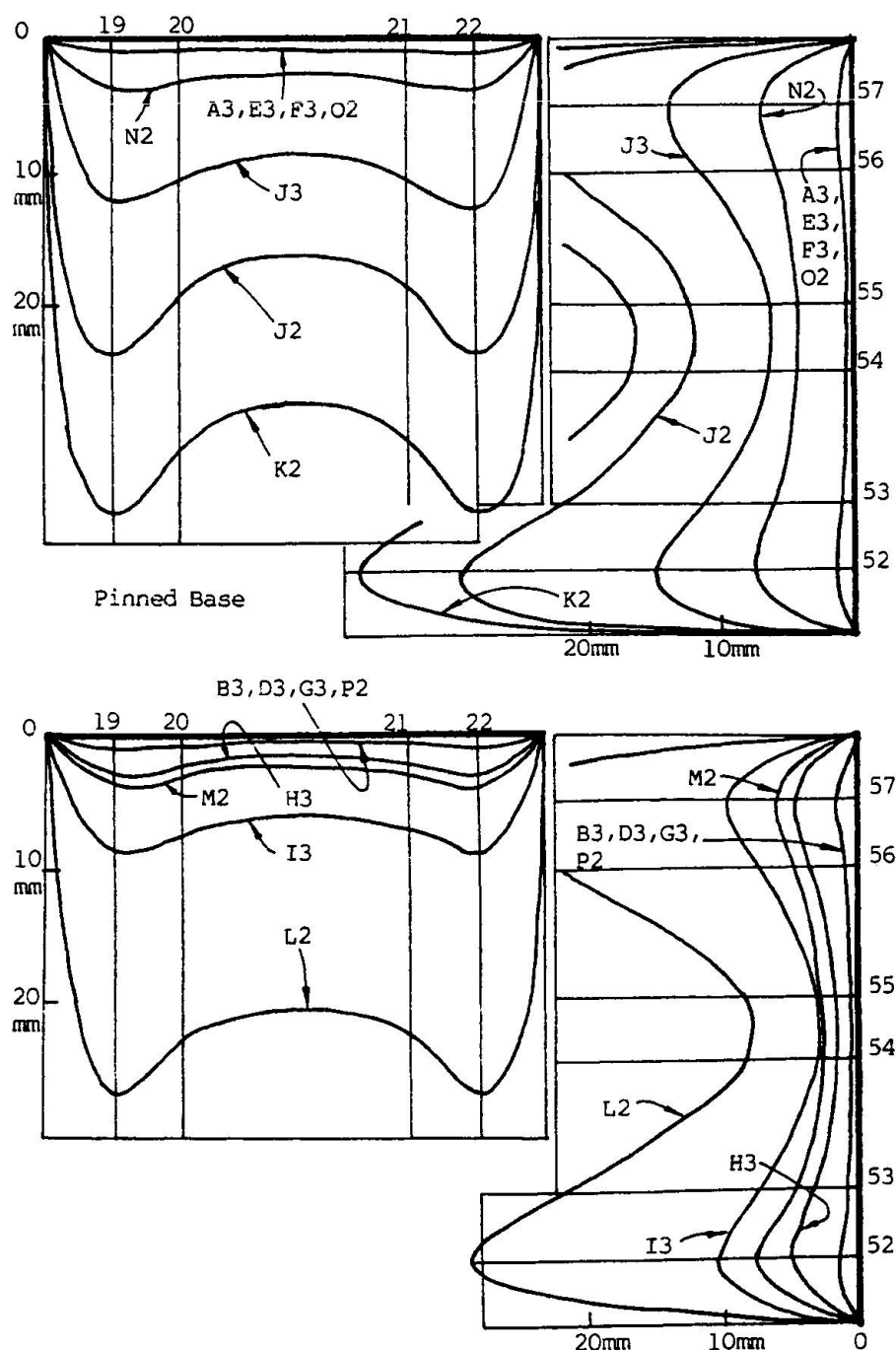


Fig. 3 Horizontal deflections along lines 19-22 and 52-57

3. RESERVE STRENGTH OF CRACKED WALLS

3.1 Assumptions of the Theoretical Analysis

As mentioned in Chapter 2, this theoretical analysis of the sheath is valid only if the thin sheath is prevented from buckling. In the previous application of the method to the vertical extension of old buildings, the masonry walls were

not damaged and this was a valid assumption. If, however, the masonry wall is cracked, then the buckling of the thin sheath is more difficult to predict, as it depends on the reserve strength of the cracked wall to which it is tied, and the lateral support it can receive from such a wall behind it.

3.2 Experimental Approach

In order to determine the reserve strength of masonry walls with diagonal cracking, model brick walls were built at a scale of 1/8 and tested to failure. The model bricks, 50 mm x 100 mm x 40 mm thick and 50 mm x 50 mm x 40 mm thick, were cut from real brick pavers with a very high compressive strength of over 48 N/sq mm. This was deliberate to ensure that failure in all cases would occur at mortar joints, as is more common in practice. A premixed, cement/lime/sand "N" mortar with a specified compressive strength of about 5 N/sq mm was used for laying the model bricks, 18 courses high, in an English bond, with mortar joints about 6-8 mm thick. With 18 courses, the test walls had dimensions of 210 mm x 50 mm x 830 mm giving a very high h/t ratio of 16.6. The purpose of a high h/t ratio was to ensure that failure of the walls in all cases occurred in compressive buckling and not in crushing. Testing was carried out in a structural steel testing frame with hydraulic actuators (jacks) applying the vertical load. To build a cracked wall, the mortar joints while still green were wire-cut in a stepped, diagonal X pattern, with three such X patterns in the wall height of 830 mm. The entire wall was thus separated into 10 sections as shown in Fig. 4. After 7 days curing the cracked wall was reassembled and tested to failure as shown in Fig. 5. The results of the tests are shown in Table 3.

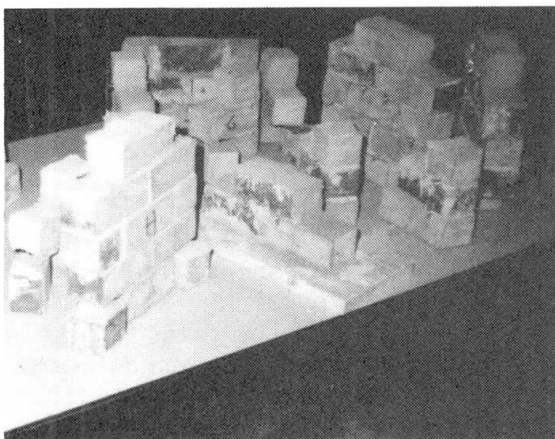


Fig. 4 Cracked wall in sections

Type of wall	Actual load kN	Load when reduced to pinned ends, kN
Uncracked	43.66	43.66
Uncracked	58.95	58.95
Uncracked	41.48	165.92
Cracked	26.20	26.20
Cracked	32.75	32.75
Cracked	21.83	21.83
With Sheath	22.92	91.68
With Sheath	25.11	100.44

Table 3 Buckling failure loads of the walls

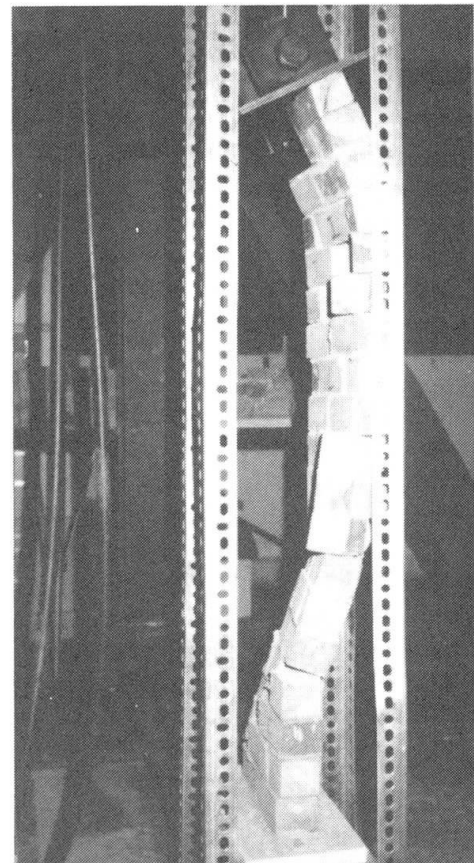


Fig. 5 Cracked wall at collapse



4. SHEATH TIED TO THE CRACKED WALL

A cracked wall was first built as described in 3.2, with, however, 34 ties embedded into the mortar. The ties were screws, 5 mm dia. and 64 mm long. Wing nuts were used when the mortar had set. Fine wire mesh reinforcement was tied to the bolt heads and the cracked wall assembled against a sheet steel form covered with plastic wrap. To prevent leakage, the wall was taped to the form; nevertheless, some leakage did occur. The wall was still a cracked wall, as seen in Fig. 6. A flowable mix was used, yet the walls still required some patching with the same grout. The thickness of the sheath varied from 6 mm, at sections where failure occurred, to a maximum of 12 mm. These walls were tested with end conditions of fixed at the base and free at the top, to stay within the load capacity of the actuator. The results are shown in Table 3.



Fig. 6 Cracked wall with sheath



Fig. 7 Sheath at collapse

5. CONCLUSIONS

This research shows that even severely damaged masonry walls can provide lateral support to the thin, reinforced concrete sheath to prevent buckling. The cracked wall has about 30% of the strength of the uncracked wall, and the provision of the sheath returns the structure to 107% of its original strength. Furthermore, whereas both uncracked and cracked walls showed explosive failure in the mortar joints, the cracked wall with the sheath showed a non-explosive failure along a single line of weakness, as shown in Fig. 7.

6. ACKNOWLEDGEMENTS

Grateful acknowledgement is made to Prof. Howard Smith of the Aerospace Engineering Dept. for the test frame and equipment, and to Dr. Dennis Domer and Dr. Tom Glavinich of Architectural Engineering for making the Structural Model Testing Laboratory operational. Also a word of thanks to Mr. Jon Lindsey, graduate student in Civil Engineering for his help in the experimental part of this research.

REFERENCES

1. LANGENBACH R., Earthquakes: A New Look at Cracked Masonry. Civil Engineering, November 1992.
2. BENJAMIN B. S., A Reinforced Concrete Sheath for Old Buildings in Poor Countries. Structural Faults and Repair-87 Conference, London, July 1987.
3. BENJAMIN B. S., Architectural and Structural Investigations of a Reinforced Concrete Space Sheath. Space Structures 4, Thomas Telford, London, 1993.

Earthquake Damage Evaluation for Reinforced Concrete Frames with Infilled Brick Walls

Dégradation de cadres en béton armé remplis de briques sous l'effet de tremblements de terre

Erdbebenschadenschätzung von Stahlbetonrahmen mit Mauerwerksausfachungen

SHEN Jumin

Professor
Tsinghua University
Beijing, China



Shen Jumin, born in 1931, received his Ph. D. degree from Moscow Civil Engineering Institute, Russia, in 1961. He is a professor of structural engineering and currently a member of Working Commission 3 "Concrete Structures" in IABSE.

SUMMARY

An efficient procedure for earthquake damage evaluation of reinforced concrete frames with infilled brick walls is presented. In analysis, the infilled brick walls can be simplified as the equivalent bracing element. The restoring force models with consideration of descending branch for reinforced concrete and infilled brick members are suggested. Pseudo-dynamic tests of two models with two stories and two spans were carried out by a computer-actuated on-line system. The analytical results obtained from elastic, inelastic and collapse response are close to those obtained from corresponding earthquake simulation.

RÉSUMÉ

L'article présente une méthode d'évaluation de la dégradation provoquée par les séismes dans les cadres en béton armé, remplis de briques. L'auteur simplifie son analyse en admettant que les bardages en briques sont équivalents à des poutres en treillis. Il propose des modèles de forces de rappel ayant une forme de branche descendante, aussi bien pour les éléments en béton armé que pour ceux en briques. Les essais pseudodynamiques réalisés ont porté sur deux modèles comportant deux étages et deux travées, soumis à l'action de vérins à commande directe par ordinateur. Les résultats analytiques découlant des comportements élastique, non élastique et à l'état ultime sont sensiblement similaires à ceux fournis par une simulation sismique correspondante.

ZUSAMMENFASSUNG

Der Artikel stellt ein Schätzungsverfahren des Erdbebenschadens für mit Mauerwerk ausgefachten Stahlbetonrahmen vor. In der Analyse werden die Füllwände als gleichwertiges Fachwerk idealisiert. Für Stahlbeton und ausfachendes Mauerwerk werden Kraft-Verschiebungsbeziehungen mit abfallendem Ast vorgeschlagen. Pseudodynamische Versuche wurden mit on-line gesteuerten Kolbenpressen an zwei Modellen mit zwei Stockwerken und zwei Feldern durchgeführt. Die analytischen Ergebnisse für das elastische, inelastische und Grenztragverhalten liegen nahe bei denen aus den entsprechenden Erdbebensimulationen.



1. INTRODUCTION

Reinforced Concrete Frames with infilled brick walls have been extensively used in seismic areas in China. The changes of actions or conversion of existing buildings to new uses often require to determine the seismic behavior of such structures. Both laboratory studies and damage observation from past earthquakes indicated that the interaction of infilled brick walls with reinforced concrete frames had a significant influence on the performance of a brick-infilled frame. However, no consensus has yet emerged to provide a unified approach for either their seismic design or load-carrying capacity and ductility evaluation. Under the strong ground motion the internal forces and deformations of the structure are usually far beyond the linear elastic range. During a severe earthquake the members may come into descending branch and the structure will be in an unstable deformation state. The previous elasto-plastic dynamic analysis methods for the multi-degree of freedom system are based on the assumption that any element in structure cannot approach the load-carrying capacity or come into the descending branch. As a result, current dynamic collapse analysis of structure is actually restricted to the stage before the ultimate state. Because the structural element in the descending branch may make the structure to come into unstable state, seismic response of the structure in the unstable state should be greatly different from the normal elasto-plastic response. It is necessary to consider an unstable state in order to evaluate correctly the damage level, weak parts and collapse process of a structure under a severe earthquake. In an infilled frame structure, the brick walls restrained by the frame act as bracings with nonlinear characteristics. Because the existence of brick infilled walls elasto-plastic seismic response of whole structure is greatly different from that of the frame without brick infilled walls.

2. ANALYTICAL METHOD OF COLLAPSE EVALUATION

In analysis the following assumptions are used:

- (1) It is assumed that the stiffness in the plane of the horizontal floor is infinite.
- (2) Trilinear degradation shape is used for representing the characteristics of the restoring force of bending moment M and curvature Φ of reinforced concrete elements as shown in Fig.1. The descending branch is considered. The degradation of unloading stiffness and reloading stiffness after unloading is also considered.
- (3) The influence of the bar slippage in joint on response of the structures is considered. The restoring force model of the slippage rotation spring at the end of the element is shown in Fig.2 [1].
- (4) When the calculation bending moment M of element reaches the yielding moment M_y , the plastic hinge zone would be formed and concentrated at the ends of the element. The element can be considered as an element of variable stiffness with nonlinear spring which represents the slippage rotation at the end of element.
- (5) The brick walls restrained by the frame act as bracings. In order to consider this interaction the brick infilled walls can be simplified as an equivalent bracing element. Based on the experimental results the restoring force model of the brick wall is suggested as shown in Fig.3 [2].

The horizontal displacement function W is assumed to be developed as following series:

$$W(s,t) = \sum_{i=1}^n T_i(t) f_i(s) \quad (1)$$

In Eq.(1) $f_i(s)$ is the horizontal unit displacement function, which describes the diagram of unit displacement of the structure and only relate with the coordination s . $T_i(t)$ is the generalized displacement function and only relate with time t .

According to the principle of virtual displacements, the equation of the virtual work of the structural system under strong ground motion can be obtained as following:

$$\sum_{i=1}^n [m_{ji} \ddot{T}_i + c_{ji} \dot{T}_i + k_{ji} T_i] = q_i \quad (2)$$

where

$$\begin{aligned} m_{ji} &= \int_0^L m f_i f_j ds \\ c_{ji} &= \int_0^L c f_i f_j ds \\ k_{ji} &= \int_0^L \frac{M_i M_j}{EI} ds + \int_0^L \frac{Q_i Q_j}{GA} ds + \int_0^L \frac{N_i N_j}{EA} ds - \int_0^L N_g f_i f_j' ds \\ q_j &= - \int_0^L m \ddot{W}_g f_j ds \end{aligned} \quad (3)$$

and \ddot{W}_g is the acceleration record of the ground motion, EI is the bending stiffness, GA is the shearing stiffness, EA is the compressive stiffness, m is the mass, c is the damping coefficient and N_g is the axial force due to the static loading. In Eq.(3), $M_i(s)$, $Q_i(s)$ and $N_i(s)$ are functions of unit bending moment, unit shearing force and unit axial force respectively. They describe the diagrams of internal forces developed under the unit displacement functions $f_i(s)$. The selection of the unit displacement functions can be arbitrary, but the relations among the unit displacement functions must be linear independent and they have to satisfy the boundary conditions. The numbers of the unit displacement functions would be determined by the degrees of freedom of the structure system. If the proportion of the response of higher modes is less in the total response of a structure system, the motion condition of the structure system under the strong ground motion can be well described by less items of the unit displacement functions. It should be pointed out that the structure will be in an unstable state as soon as the stiffness matrix of the whole structural system has any non-positive eigenvalue. The definition about the structure collapse under a severe earthquake may be represented as following: if the structure has been in unstable state and, at the same time, the ductilities of the structure approach concerned value, the structure collapses[3]. From this definition the unstable state of the structure is necessary condition for the structure collapse.

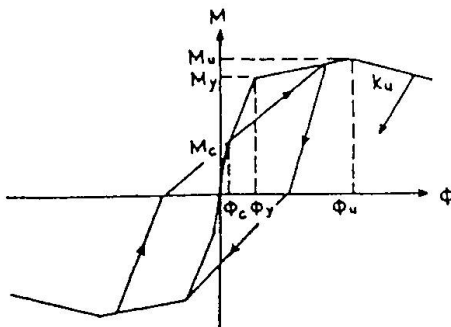


Fig.1

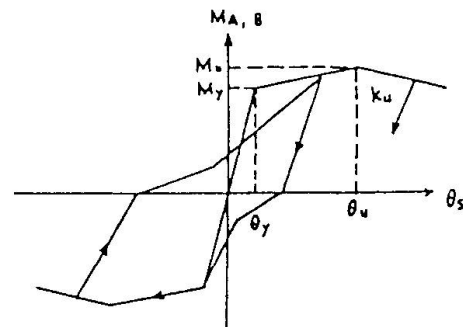


Fig.2

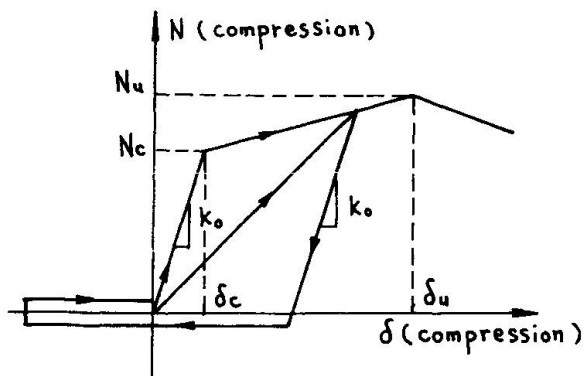


Fig.3

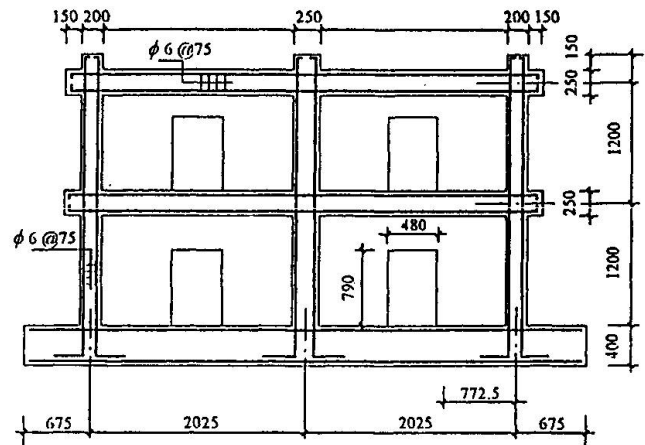


Fig.4

3. EXPERIMENTAL VERIFICATION BY PSEUDO-DYNAMIC TEST

In order to gain a better understanding of seismic behavior of brick-infilled reinforced concrete frames and to verify the mechanical model and analysis method, three frame models were tested by computer-actuator on-line system [4,5]. Three models with infilled brick walls fully, with infilled brick walls having openings and without infilled walls were made. Designations of three test models are used as FFW, FWO and FNW respectively. The dimensions of three models with two stories and two spans are in 1:2.5 scale of the prototype structure. Figure 4 shows the overall dimensions of the three models. The dimension of bricks is $120 \times 57 \times 53$ mm, which were cut out from normal bricks with dimension of $240 \times 115 \times 57$ mm. The sections of columns and girders are 20×20 cm and 15×25 cm respectively. Ground acceleration for earthquake simulation was modelled after the N-S component of EL Centro 1940 earthquake. Figure 5 shows the maximum base shear force of the three models in the different experiment stages. It can be seen from the figures that the differences in the seismic response of the three models are apparent and reasonable. For model FFW during simulation with peak base acceleration $0.2g$ the visible crack appeared in infilled wells. During simulation with peak base acceleration $0.4g$, the cracks in infilled wall widened and developed toward the corner of the wall and connected to form major X shape diagonal crack, and the reinforcing bars in the middle column of the first story yielded with

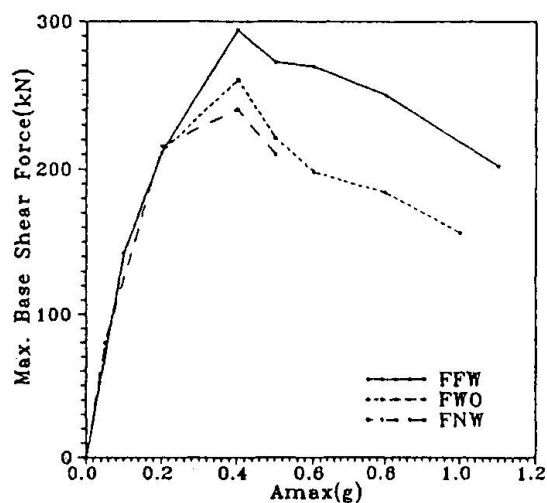


Fig.5

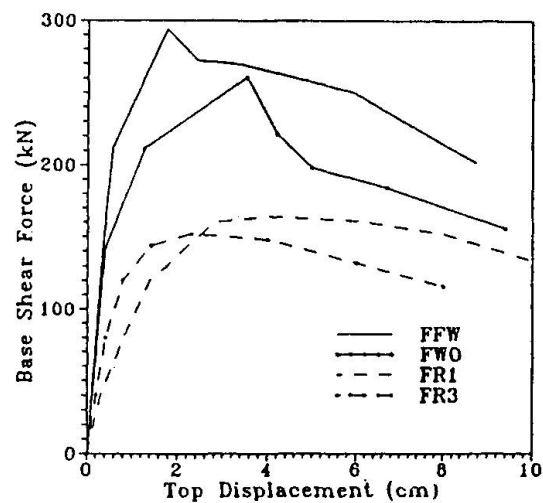


Fig.6

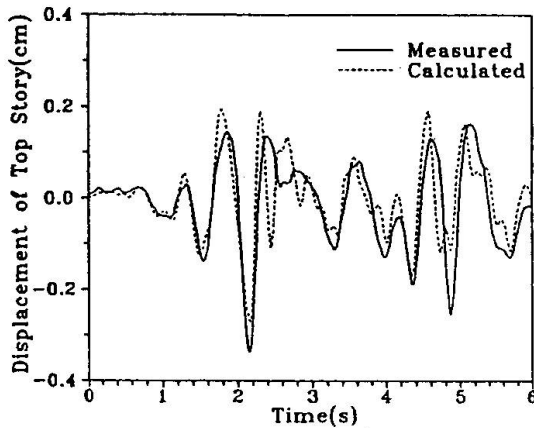


Fig.7 Elastic Response ($A_{\max}=0.1g$)

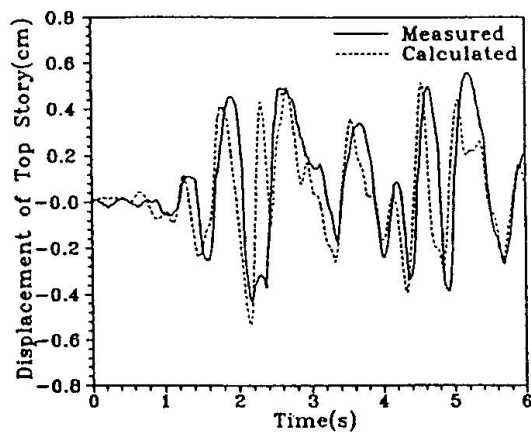


Fig.8 Inelastic Response ($A_{\max}=0.2g$)

great decrease of the structure stiffness so the structure reached yielding stage. During simulation with peak base acceleration 1.1g the structure suffered a serious damage in the first story, but the top story suffered much less serious damage. For model FWO during simulation with peak base acceleration 0.2g the previous cracks developed toward the corner of infilled walls and the X shape diagonal cracks formed in both sides of openings. During simulation in which peak base acceleration were 0.4g and 1.0g respectively, the structure reached yielding stage and failure stage respectively. The most serious damage occurred around openings and at the ends of columns in the first story. The load-carry capacity of model FNW is much less than that of models FFW and FWO. Fig.6 Shows the measured relation between base shear force and top displacement for models FFW, FWO, FR1 and FR3 in different experiment stages. The models FR1 and FR3 at same size with models FFW and FWO were tested by quasi-static method [6]. The model FR1 and FR3 were designed as a strong column-weak beam type and strong beam-weak column type without infilled walls respectively. The damage and deformation of FWO was more serious than that of model FFW.

The measured and calculated time-dependent curves of displacement for model FFW during simulation with peak base acceleration 0.1g and 0.2g are shown in Fig.7 and Fig.8 respectively. Figure 9 shows the measured and calculated time-dependent curves of displacement for model FFW during simulation with peak base acceleration 1.1g. The calculated curve is obtained by inelastic analysis with consideration of descending branch. It is indicated that the experimental and analytical results in elastic, inelastic and collapse earthquake response are in good agreement.

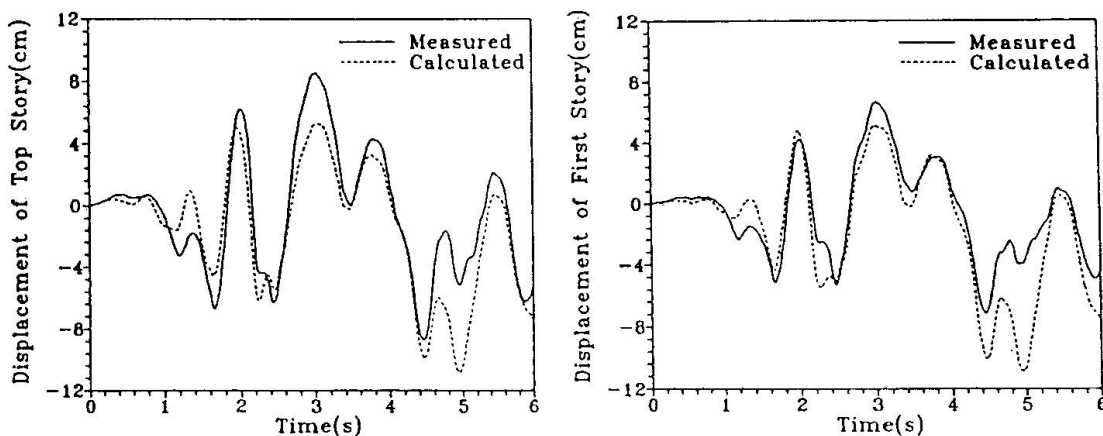


Fig.9 Collapse Response ($A_{\max}=1.1g$)



4. CONCLUSIONS

1. From experimental and analytical results it is shown that due to the existence of the infilled brick walls the initial stiffness and load-carry capacity of a frame obviously increase, but the deformation capacity and ductility of both frames with or without infilled walls are nearly same. The inelastic earthquake response of whole structure with infilled brick walls is greatly different from that of the frame without infilled brick walls.
2. The plastic hinges of a brick infilled frame may appear at the ends of columns under strong ground motion.
3. The measured and calculated time-dependent curves of displacement of infilled-brick frame without openings, whether in the elastic stage, inelastic stage or in failure stage after the structure comes into the unstable stage, are all in good agreement. It is indicated that the mechanical models, restoring force model and calculated method in analysis are reasonable.

ACKNOWLEDGMENTS

This work was undertaken in Institute of Structural Engineering of Tsinghua University. The assistance of Mr. Wang Daging and Zhu Ronghua is gratefully acknowledged.

REFERENCES

- [1] Shen Jumin, Weng Yijun & Feng Shiping, Behavior of R/C Compression-Flexure Members Under Cyclic Loading, China Civil Engineering Journal, Vol.15, No.2, 1982, pp.53-64.
- [2] Wang Daqing, Earthquake Collapse Analysis of Reinforced Concrete Frame Structure with Infilled Brick Walls, Master Thesis, Department of Civil Engineering, Tsinghua University, Beijing, China, 1991.
- [3] Feng Shiping & Shen Jumin, Collapse Earthquake Response of Reinforced Concrete Frame Structures, Earthquake Engineering and Engineering Vibration, Vol.9, No.1, 1989, pp.67-78.
- [4] Yin Wenduo, Earthquake Response Analysis of R/C Frame in Computer-Actuator On-Line System, Master Thesis, Department of Civil Engineering, Tsinghua University, Beijing, China, 1988.
- [5] Rhu Ronghua, Earthquake Response Simulation of Reinforced Concrete Frames with Brick Infilled walls by Pseudo-Dynamic Test. Master Thesis, Department of Civil Engineering, Tsinghua University, Beijing, China, 1994.
- [6] Shen Jumin, Feng Shiping & Weng Yijun, Inelastic Behavior of Reinforced Concrete Frame Subjected to Reversal Cyclic Loading, Proceedings of US-PRC Joint Workshop on Seismic Resistance of Masonry Structures, Harbin, China, 1986.

Study of a Multi-Storey Brick Infilled Reinforced Concrete Structure

Etude d'une structure à plusieurs étages en béton armé remplie de briques

Untersuchung von mehrstöckigen Stahlbetonkonstruktionen mit
Ziegelsteinausfachung

E.B. Perumal PILLAI

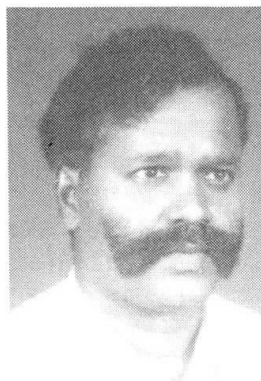
Lecturer
Coimbatore Inst. of Technology
Coimbatore, India



E.B.P. Pillai, born 1960, received his B.E. and M.E. Degrees from CIT of Madras University. He is now doing his Ph.D. thesis on reinforced concrete and infilled frames.

P. GOVINDAN

Assistant Professor
Coimbatore Inst. of Technology
Coimbatore, India



P. Govindan, born 1954, received his B.E. and M.E. Degrees from CIT of Madras University. He obtained his Ph.D. from Anna University, Madras. His research includes infilled frames.

SUMMARY

The behaviour of two multi-storey, reinforced concrete frames, with brick infill and without, was studied experimentally. The failure modes of both the frames and the effect of brick infill in multi-storey multi-bay infilled frames were assessed. The strength, stiffness, ductility and energy absorption characteristics of both the frames are discussed in this paper.

RÉSUMÉ

Le comportement de deux structures à plusieurs étages, en béton armé, - l'une remplie de briques et l'autre sans briques - a fait l'objet d'une étude expérimentale. Le mode de rupture des deux charpentes et l'effet de la présence ou de l'absence des briques été étudié. La résistance, la rigidité, la ductilité, et la capacité d'absorption de l'énergie des deux charpentes sont discutés dans cet article.

ZUSAMMENFASSUNG

Das Verhalten von zwei, mehrstöckigen Stahl-Betonrahmen werden untersucht. Einer davon ist ohne Ziegelsteinausfachung und der andere ist mit Ausfachung. Die Art des Versagens wird für die beiden Rahmen abgeschätzt. Die Eigenschaften der Festigkeit, der Steifigkeit, der Duktilität und der Energieaufnahme von diesen Rahmen werden hier diskutiert.



1. INTRODUCTION

A recent United Nations study estimates the world population by the year 2000 A.D. to exceed six billions and that the urban population will be half of the world's total population. With the population explosion and increase in land prices sky rocketing, sky scrapers have become the necessity of the present day. In tall structures, the inplane horizontal loads are a matter of great concern and need extraordinary consideration in the design of multistorey buildings. One method of resisting lateral load is considering the structural stiffness and strength of masonry infill walls. Liauw and Lo [1] and Klinger and Bertero [2] have studied experimentally the factors affecting the stiffness and ultimate load of multibay and multistorey infilled frames.

The object of present investigation is to quantify the parameters like load carrying capacity, stiffness, ductility and energy absorption capacity for a two-bay R.C. frame with and without infill.

2. BASIS OF DESIGN

The elasto-plastic analysis based on beam hinge mechanism was assumed. It has been further assumed [3] that plastic hinges form in all floor beams in both bays before plastic deformation of any kind would occur in any of the columns of reinforced concrete frame without brick infill. The dimensions were fixed using quarter scale and the beams and column sections for the model are shown in Fig.1.a and Fig.1.b. The reinforcement details are shown in Fig.2.

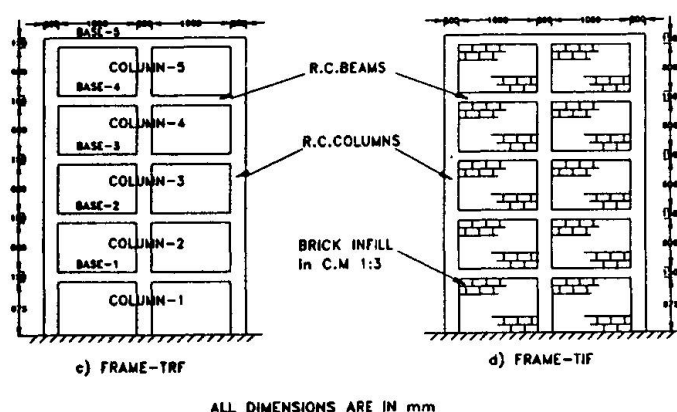


FIG.1 QUARTER SIZE FIVE STOREY TEST SPECIMENS

3. NUMERICAL SOLUTION

The two-bay infilled frame is analysed by replacing the infill as equivalent strut.[4]. The infilled frame was idealized as a pin jointed truss neglecting bending moments in beams and

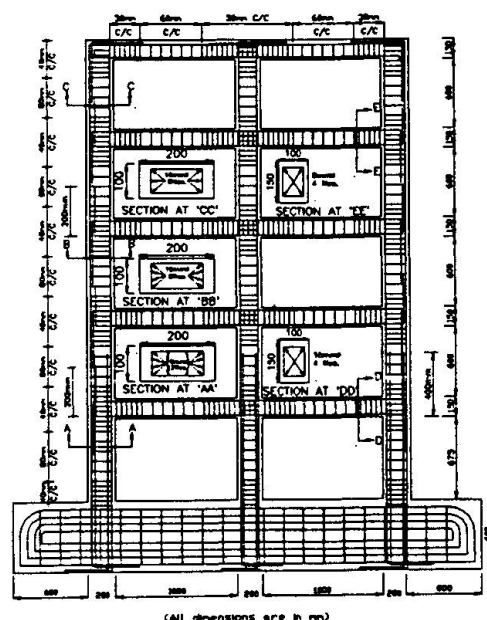


FIG.2. SCHEMATIC DIAGRAM OF REINFORCEMENT DETAILS

columns. Using strain energy concept, the forces in different members were determined and the values are shown in Fig.3.a. The collapse base shear works out to 412.338 kN. In the other method, the frame was assumed as a rigid-jointed framework, taking into consideration the bending moments also. The forces and moments calculated are given in Fig.3.b. The calculated ultimate base shear was found to be 444.819 kN.

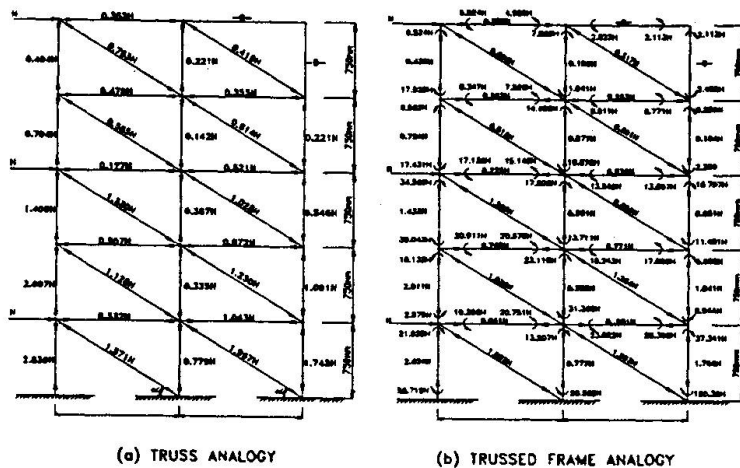


FIG.3 NUMERICAL SOLUTION

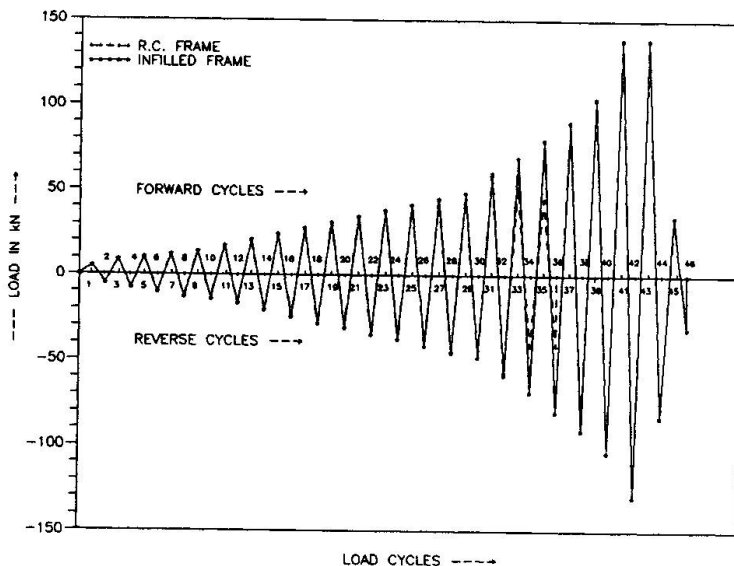


FIG.4 LOAD SEQUENCE FOR FRAMES TRF AND TIF

4. TESTING PROCEDURE

Three load points were located at fifth storey, third storey and first storey levels. Using hand operated oil pumps and double acting jacks, static reversed cyclic lateral load was applied. The loading sequence in the beginning for both frames were identical as shown in Fig.4. Near final collapse, the increment of load was controlled based on visible deformation capacity of the frames.

5. EXPERIMENTAL RESULTS AND COMPARISON

5.1. Load Vs. Deflection

The lateral deflection of the frames at all the five storey levels were measured and the displacement due to rigid body rotation of the footing and the foundation block were incorporated in the calculation of net deflection. The deflection at top storey level with respect to maximum base shear of each cycle for frame-TIF is shown in Fig.5. The deflections at later cycles were greater than that in the preceding cycles.

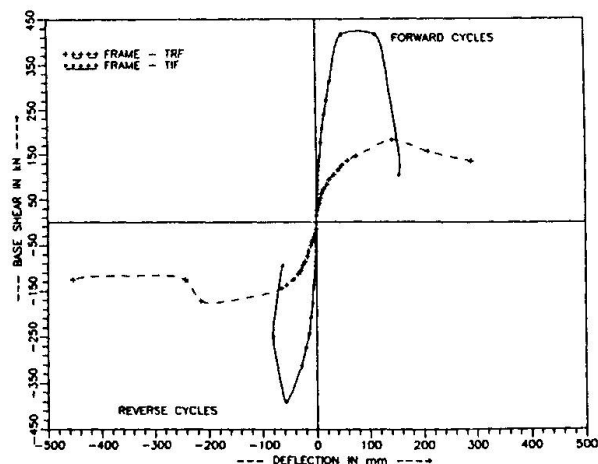


FIG.5. BASE SHEAR VS TOP STOREY DEFLECTION FOR FRAMES TRF AND TIF



5.2. Stiffness

The stiffness of both the frames is defined here as the base shear required to cause unit deflection at the top storey level. In both the frames TRF and TIF there was general degradation of stiffness with respect to increase in load cycles as can be seen from Fig.6. The stiffness of frame-TIF was always greater than that of frame-TRF during all stages of loading.

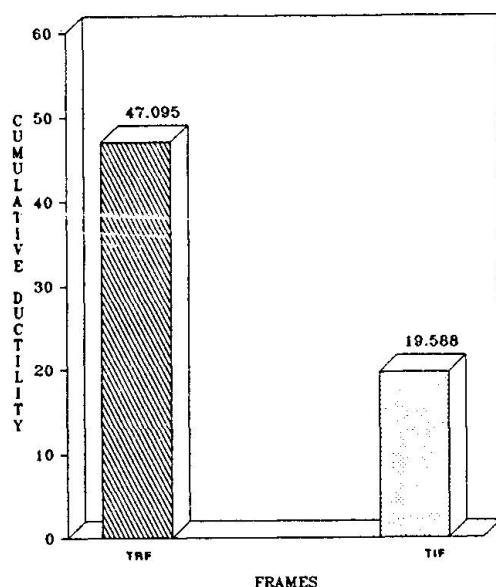


FIG.7 COMPARISON OF CUMULATIVE DUCTILITY

5.4. Energy Dissipation

It is important for a building in a seismic zone to be resilient, i.e. absorb the shock from the ground and dissipate this energy uniformly throughout the structure. The proportionate energy dissipation during various load cycles was calculated as the sum of the areas under the hysteresis loop. The cumulative energy dissipated by the frame-TRF is 167.6 kN-m in thirty six cycles whereas the total energy dissipated by the frame-TIF was 110.633 kN-m. The cumulative energy dissipated for both frames are shown in Fig.8.

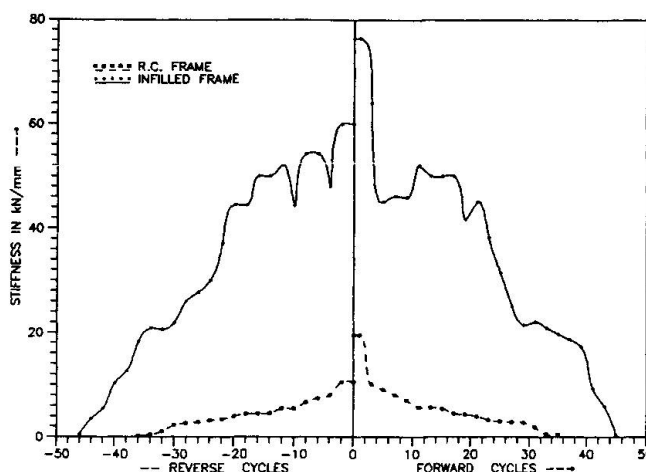


FIG.6 COMPARISON OF STIFFNESS FOR FRAMES TRF AND TIF

5.3. Ductility Factor

The ductility factors for the frames are calculated as the ratio of maximum deflection at any load level and the first yield deflection. The yield deflection is obtained by assuming bi-linear behaviour of the frames. The yield deflection for frame TRF is 21.0 mm and for frame TIF is 13.6 mm. The ductility factor values for various load cycles of the specimens were worked out and the cumulative ductility factor for both the frames are calculated and given in Fig.7.

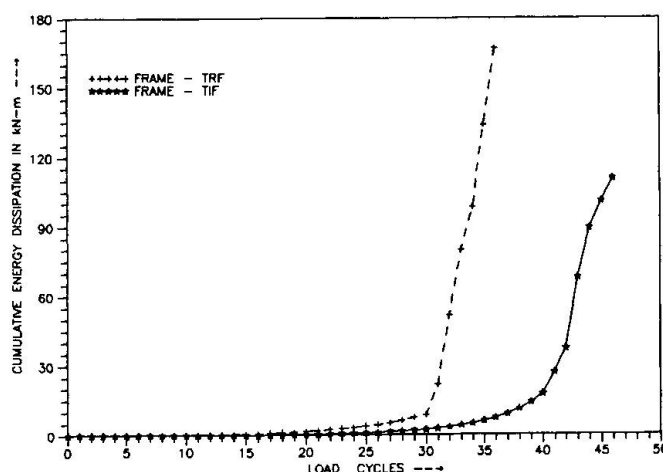


FIG.8. COMPARISON OF CUMULATIVE ENERGY DISSIPATION CAPACITY

5.5. Mode of Failure

In bare frame, the crack width increased when the load is increased further and further. The steel in floor beams got yielded due to excessive deformation of the structure (Fig.9). After all the floor beams plastified, the windward column steel yielded and crushing of concrete took place in leeward column and then in the middle column.

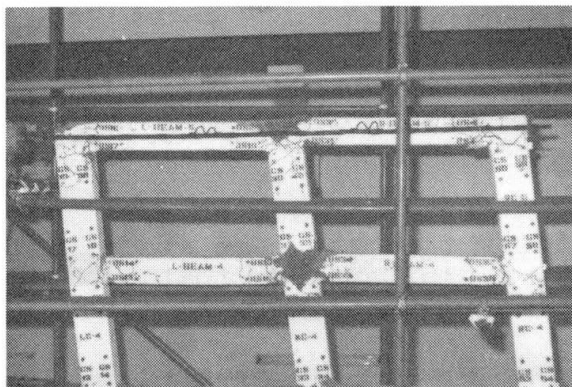


FIG.9. FAILURE OF FRAME -TRF

In frame-TIF, it is seen that the infill cracked along the bed joints as well as along the diagonal. During the reverse cycle, the cracks, which formed during the forward cycle, closed and new cracks developed across the tension diagonal of the brick panel. The cracking which occurred during forward and reversed cycles reflect the fact that the infilled frame behaved as an integral unit. At failure the frame-TIF exhibited spalling of brick fragments as shown in Fig.10.

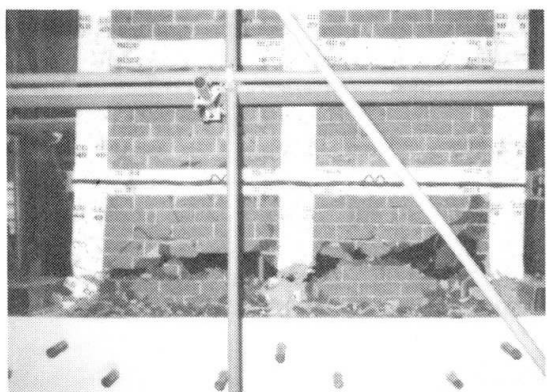


FIG.10. SPALLING OF BRICKS

The damaged brick infill is likely to cause flying fragments in the case of infilled walls and needs protection. The complete failure of the Frames TRF and TIF are shown in Fig.11 and Fig.12.

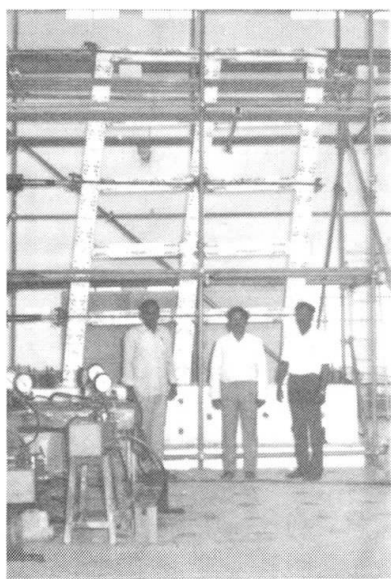


FIG.11. FRAME - TRF AT FAILURE

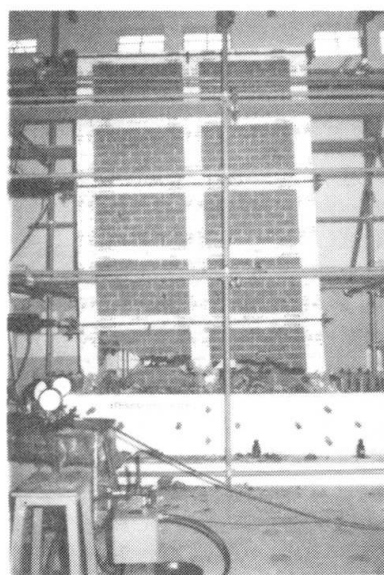


FIG.12. FRAME - TIF AT FAILURE



6. CONCLUSIONS

1. The load capacity of infilled frame increases by 2.29 times as that of bare frame. The initial cracking load of infilled frame is 2.5 times more than that of the bare frame.

2. In the initial stage, the infilled frame is 3.93 times stiffer than the bare frame. The stiffness of infilled frame is always greater than that of bare frame during all stages and all cycles of loading.

3. The R.C. frame is 1.73 times more ductile than the infilled frame. The R.C. frame can absorb 1.51 times more energy than the infilled frame.

4. As the stiffness of the infilled frame is higher than that of the bare frame, larger load is being resisted. It is to be noted that the frame TRF is designed as a bare frame and hence this type of enormous stiffness will mean that unduly large forces are to be resisted by the infilled frame. This may even cause rigid body movements at foundation levels endangering the stability of the whole structure.

5. The behaviour and failure mechanism of bare frame are different from that of the infilled frame. In infilled frame plastic hinge hinges did not form in all the beams before column hinges developed whereas in the R.C. frame, plastic hinges formed in all beams before final collapse of the frame.

7. ACKNOWLEDGEMENT

The authors are grateful to the Management, the Principal, Head of the Department and other Faculty members of C.I.T., Coimbatore, India. The financial assistance provided by the Ministry of Human Resources Development, India, is gratefully acknowledged.

8. REFERENCES

1. LIAUW, T.C., and LO, C.Q., 'Multibay Infilled Frames Without Shear Connectors', Journal of American Concrete Institute, Vol.85, No.4, Jul-Aug.1988, pp 423-428.
2. KLINGER, R.E., and BERTERO, V.V., 'Earthquake Resistance of Infilled Frames', Journal of Structural Division, ASCE, Vol.104, No.6, June 1978, pp 973-989.
3. PAULAY, T., and SANTHAKUMAR, A.R., 'Ductile Behaviour of Coupled Shear Walls', Journal of Structural Division, ASCE, Vol.102, Jan.1976, pp 93-108.
4. SMITH, B.S., and CARTER, C., 'A Method for Analysis of Infilled Frames', Proceedings of The Institution of Civil Engineers, Vol.44, Sept. 1969, pp 31-48.

Structural Rehabilitation with Advanced Composites

Réhabilitation des structures porteuses avec des matériaux composites
d'avant-garde

Sanierung von Tragwerken mit modernen Verbundwerkstoffen

Frieder SEIBLE

Professor

Univ. of California, San Diego
La Jolla, CA, USA



Frieder Seible received his civil engineering degrees from the Universities of Stuttgart, Calgary and Berkeley. He is director of the Powell Structural Research Laboratories. His research focus is on seismic design and retrofitting of bridges, large scale experimental testing and the application of advanced composites in civil engineering.

SUMMARY

The paper provides an overview of the use of advanced composites in the repair, strengthening and seismic retrofit of existing concrete structures. The structural effectiveness of these rehabilitation measures is documented by large-scale experimental data in direct comparison to tested "as-built" behaviour and conventional rehabilitation measures. Advantages of and concerns with the uses of these new materials in civil engineering applications are addressed.

RÉSUMÉ

Cette communication donne une vue synoptique sur l'utilisation de matériaux composites d'avant-garde et hautement performants, pour renforcer et réhabiliter les ouvrages en béton. L'efficacité structurale de ces mesures de rénovation repose sur d'innombrables données résultant d'essais réalisés à grande échelle; ces données sont comparées aux résultats expérimentaux effectués sur des ouvrages existants et aux méthodes de réhabilitation classiques. Les avantages et les incertitudes découlant de l'emploi de ces nouveaux matériaux dans le domaine des constructions civiles sont présentés.

ZUSAMMENFASSUNG

Der Beitrag enthält einen Überblick über die Anwendung von hochfesten Kunstfasern in der Reparatur, Verstärkung und Erdbebensicherung bestehender Betonbauten. Die konstruktive Wirksamkeit dieser Erneuerungsmassnahmen ist mit Grossversuchsergebnissen dokumentiert und mit Versuchsdaten von bestehenden Bauten und konventionellen Sanierungsmethoden verglichen worden. Die Vorteile und Bedenken, die aus der Anwendung dieser neuen Materialien im Bauingenieurbereich erwachsen, werden erörtert.



1. INTRODUCTION

Advanced composite materials, predominantly developed for use in the aerospace industry, have shown a great potential for strengthening, retrofitting and repair of existing buildings and bridge structures to extend their service life well into the 21st century. With the broader availability of glass, aramid and carbon fibers, as well as automation in the manufacturing process, PMCs (Polymer Matrix Composites) can be affordable and competitive with conventional structural rehabilitation materials and processes.

The structural effectiveness of PMCs in rehabilitating existing structural systems has repeatedly been demonstrated with full or large-scale structural tests at the University of California, San Diego. Carbon fabric overlays have been used to retrofit reinforced and unreinforced masonry walls for seismic loads and to restore and more than double the displacement capacity in the repair of a full-scale 5-story reinforced masonry building tested under simulated seismic loads to failure. Bridge columns were seismically retrofitted and repaired with fiberglass, carbon and hybrid composite jackets and composite retrofits were shown to be just as effective as conventional steel jacket column retrofit technology.

While the low density and the high mechanical characteristics of advanced composite materials were long recognized, applications in the civil engineering sector were limited to date due to (1) high materials and manufacturing costs, and (2) the component by component replacement of existing structural members rather than a comprehensive design approach with these new materials. This paper provides an overview of the use of advanced composites in the repair, strengthening and retrofit of existing civil structures.

2. ADVANCED COMPOSITES FOR CIVIL ENGINEERING APPLICATIONS

The most common advanced composites fibers used in PMC structural applications are carbon, aramid and glass, and the most commonly used matrices are epoxies and esters. While a detailed discussion of materials, and manufacturing processes of these PMCs can be found elsewhere [1], only their key characteristics, including cost, will be summarized here with direct reference to civil engineering applications. In order to compete with conventional civil engineering materials, often referred to high performance fibers developed and used in the aerospace industry are cost prohibitive in the civil sector, limiting the choice to advanced composite materials referred to under the low to medium performance category.

The range of realistic properties can be summarized as follows:

strength: For quasi-isotropic material considerations or design assumptions strength values comparable to high strength structural steels can be achieved. However, due to the non-ductile failure characteristics only a limited range of these capacities can be utilized. Uni-directional fiber geometry can result in strength characteristics similar to high strength prestressing wires and strands.

strain: Failure strains are low and typically limited to the 1 to 3% range with carbon fibers at the lower and glass and aramids at the upper end of the range.

modulus: Moduli for quasi-isotropic assumptions range from 10% to 30% of steel and for uni-directional fiber applications from 1/3 to 2/3 of the structural steel modulus.

cost: Cost is dominated by the price of the fiber material, ranging currently per pound from \$1-3 for glass to \$10-14 for carbon (T300, AS4). Typical resins are \$1-2 per pound.

With a 40 to 60% typical fiber volume fraction and automated manufacturing techniques, PMC structural component costs in place can range from \$3-12 per pound, with glass at the lower and carbon at the upper end of the range.

It should be noted that both strength and modulus decrease rapidly with deviation of the fiber orientation from the loading direction which is largely a function of a very low shear modulus of the matrix or resin system, typically 1% or less of Young's Modulus for steel. For rehabilitation of existing concrete structures, the reduced weight of these advanced composite materials is not an issue since the application consists of thin overlays, as will be discussed in the following.

While the chemical resistance of these PMCs to acid or corrosive environments is very good in general, durability aspects such as ultra violet degradation of the matrix, alkaline reactions between glass and concrete, and water absorption by the resin system typically require a form of protective external coating. Furthermore, only limited information on the creep and relaxation characteristics of affordable PMCs in the civil engineering environment exist to date and require comprehensive evaluations. Also, significant differences in thermal characteristics between the existing concrete substrate and the PMC overlays need to be addressed. In the following only the short term structural effectiveness of PMC rehabilitation of existing concrete structures is discussed.

3. REHABILITATION OF EXISTING CONCRETE STRUCTURES

Rehabilitation of existing concrete structures with PMCs can be accomplished in three ways, namely by (1) external post-tensioning with PMC systems, (2) by linear application of strips of PMCs bonded and anchored to the concrete members, and (3) by thin surface overlays.

The first two general applications have been successfully implemented e.g. Meier, et al [2], but require the transfer of localized forces from the composite system to the existing structure. This need for special anchorage devices and local concentrated force transfer can largely be eliminated through the use of distributed surface overlays. Over the past five years these structural surface overlays have been systematically developed at UCSD and applied to (1) the seismic retrofit and repair of bridge columns, (2) the seismic retrofit and strengthening of reinforced and unreinforced concrete and masonry walls, and (3) the strengthening of bridge structures for increased superstructure capacity. Due to increasing concerns with the alkaline reaction between concrete and glass, the research described in the following has primarily focused on carbon overlays which are chemically and environmentally more resilient and stable.

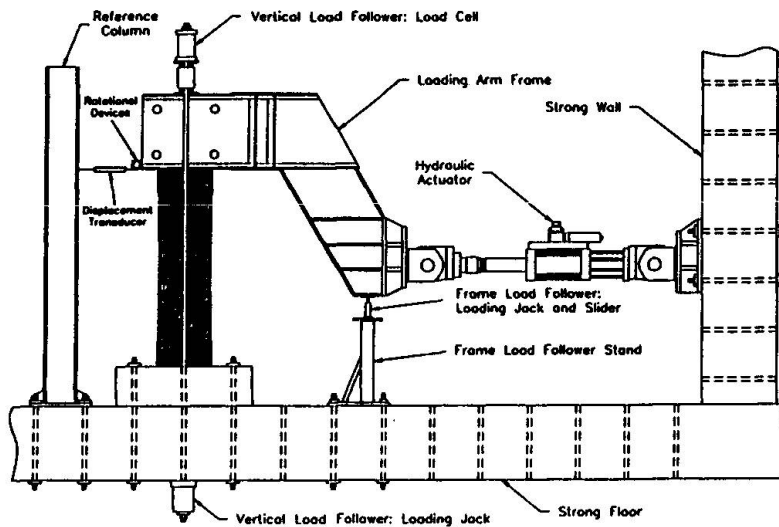
3.1 Seismic Retrofit and Strengthening of Columns

One of the primary deficiencies of older reinforced concrete columns both in bridges and buildings is the insufficient amount of transverse reinforcement. Problems arising from this deficiency are (1) low ductility in unconfined concrete with low ultimate strength and strain, (2) premature buckling of longitudinal column reinforcement, (3) shear failures, and (4) bond and development failures of lap spliced reinforcement.

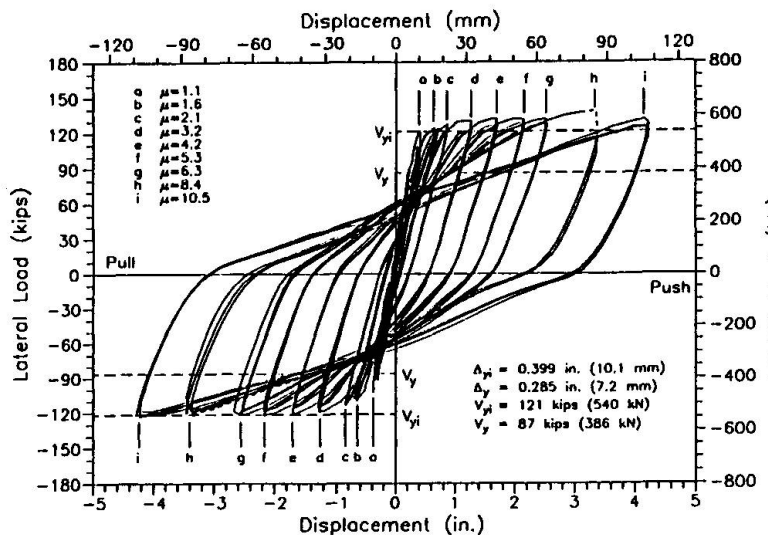
All of the above deficiencies can be removed by jacketing of the existing concrete column preferably with a circular or oval jacket providing distributed confining forces which result from the jacket curvature once membrane action in the jacket is activated by column dilation. For shear, which is not so much a confinement but rather a strength issue, also jackets of rectangular



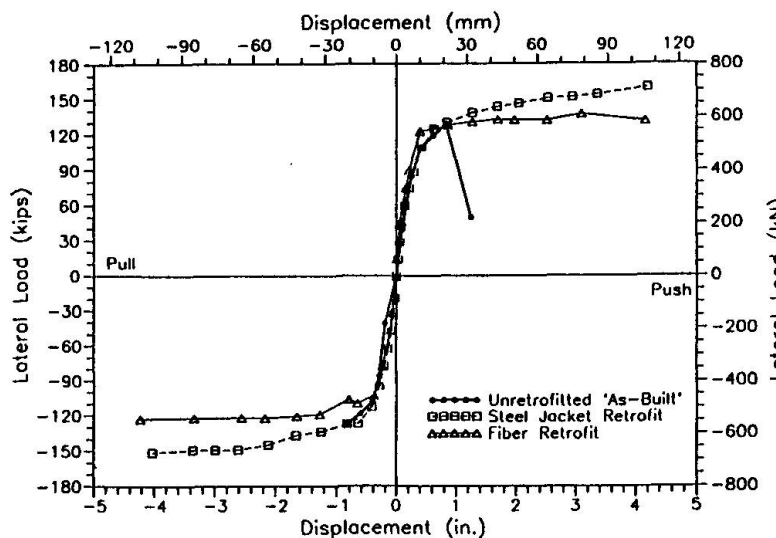
Fig. 1 Automated Carbon Jacket System



a) Test Setup



b) Load-Displacement Hysteresis



c) Load-Displacement Envelope Comparison

Fig. 2 Carbon Jacket Retrofitted Shear Column Test

geometry can be very effective. General repair and retrofit principles developed by Priestley, et al [3] apply and can directly be used to design carbon jackets. In order to compete with widely used steel jacketing, an automated winding system with 12k prepreg carbon tows was developed and tested under an Advanced Research Projects Agency (ARPA) technology reinvestment project by the Advanced Composite Technology Transfer Consortium to retrofit prismatic columns of circular, oval or rectangular cross-section. The automated winding system is depicted in Fig. 1, during the jacket installation on a rectangular bridge column model. The effectiveness of the carbon jacket system is demonstrated in Fig. 2 with the example of a circular shear column tested in double bending as shown in Fig. 2a to a displacement ductility of over ten with stable hysteretic behavior, see Fig. 2b. A direct comparison of the load-deflection envelope with tests of a corresponding unretrofitted "as-built" column and a steel jacket retrofitted column is presented in Fig. 2c and shows that not only the same ductility provided by the steel jacket was reached, but that this ductility was achieved without strength or stiffness increase which are phenomena to be avoided during seismic column retrofit [4]. The first prototype field demonstrations of this retrofit technology are currently in progress in cooperation with Caltrans in Los Angeles and San Diego.

3.2 Structural Wall Overlays

Seismic repair and retrofitting of structural walls can be accomplished very economically with thin advanced composite wall overlays. Tests have focused to date on (1) reduction of shear deformations in seismically damaged structural walls, (2) retrofitting of shear walls to achieve ductile flexural in-plane behavior, (3) increase in flexural ductility of structural walls, as well as (4) retrofitting of out-of-plane unreinforced structural walls.

A series of seven single-story structural wall panel tests were

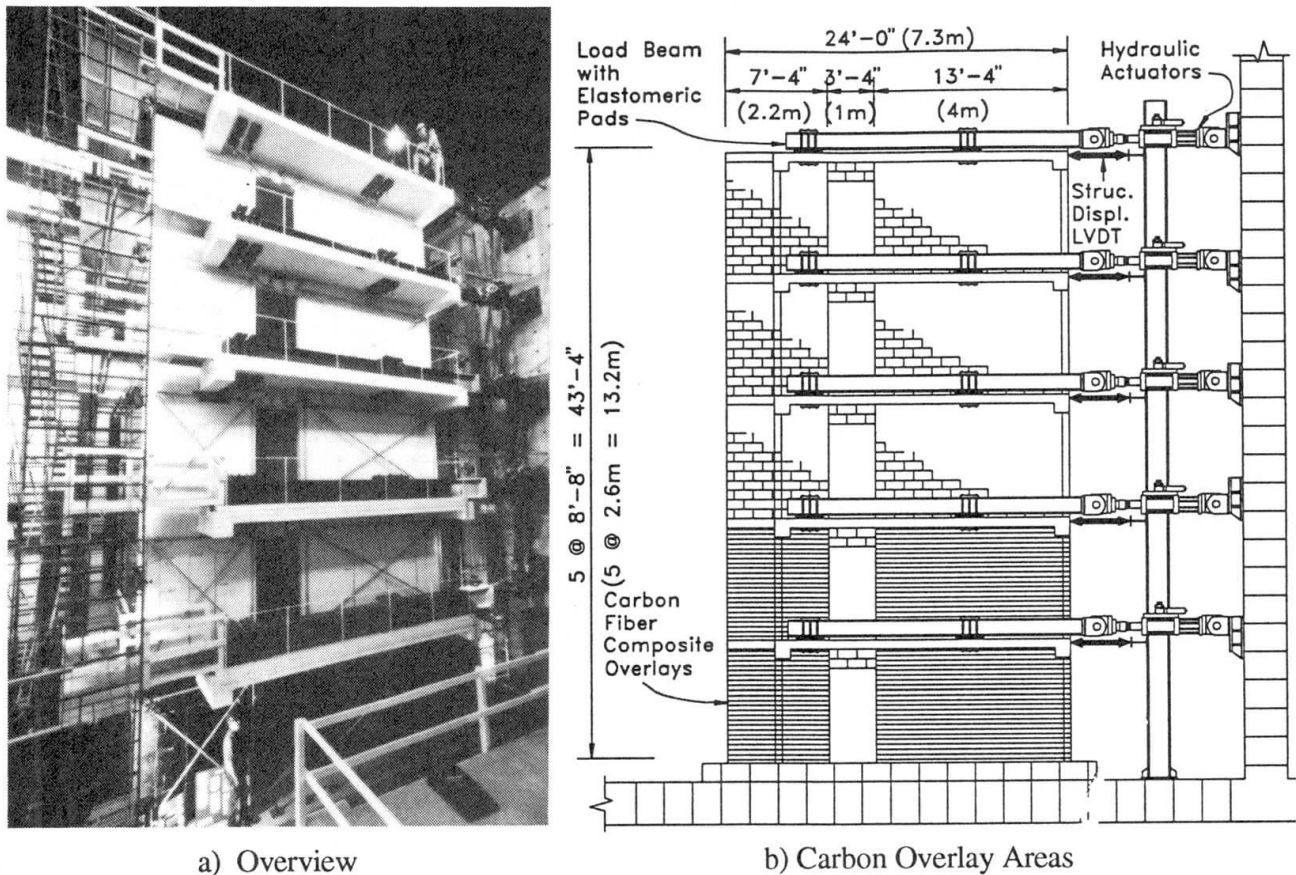


Fig. 3 Five-Story Full-Scale Building Test

performed on fully grouted hollow core concrete masonry walls at full-scale. Subsequent to sandblasting and filling of voids with epoxy or polymer concrete, advanced composite overlays are applied to the wall surface either single or double-sided in the form of mats or woven fabrics saturated with resin in an impregnator.

Especially for in-plane wall response or shear, very thin overlays (only one or two layers $t_i = 0.5$ to 1.0 mm) can show significant seismic improvements. Composite fibers are oriented horizontally to cross diagonal or shear cracks, while allowing horizontal or flexural cracks to open. Forces to be transferred in the composite overlays are limited by the laminar shear or principal tensile strength of the existing structural wall material since the polymer resin typically features significantly higher tensile capacities than the concrete or masonry substrate.

To improve shear capacities of structural walls of length d with advanced composite overlays of thickness t_o and a conservative diagonal tension crack angle assumption of 45° , the resulting shear capacity increase can be determined as

$$V_o = f_o t_o d \quad (1)$$

where the allowable overlay stress level f_o is based on a maximum allowable strain of 0.004 above which aggregated interlock is assumed to be lost.

However, for typical structural wall aspect ratios, i.e. height and length of approximately the same dimensions, the above strain criteria inherently assumes large shear deformations, namely 0.4% drift due to shear alone in order for the composite overlay to become effective. Thus, additional limitations on the total allowable shear deformations can be imposed by reducing the allowable



overlay stress level f_o . Alternatively, stiffness criteria can be employed in the wall overlay design, limiting shear deformations to deformation levels which can be expected in concrete walls with conventional horizontal reinforcement $A_{sh}^{req.}$ (determined based on conventional design requirements), by scaling the amount of horizontal overlay fabric A_{oh} from the required horizontal reinforcement as

$$A_{oh} = A_{sh}^{req.} \frac{E_s}{E_o} \quad (2)$$

which will also ensure equal participation of the already existing conventional horizontal wall reinforcement.

Since the bond between the composite overlays or the resin matrix and the concrete substrate is at least as good as the bond capacity between individual reinforcing bars and unconfined concrete, upper limits to the total improvement of shear capacity can also be taken as those encountered in conventional concrete design codes.

The seismic deformation limitations of many structural walls are controlled by compression toe crushing or lateral stability of the compression toe region. A nominal level of compression toe confinement can be provided by wrapping additional layers of composite overlay material around the toe region if access is available.

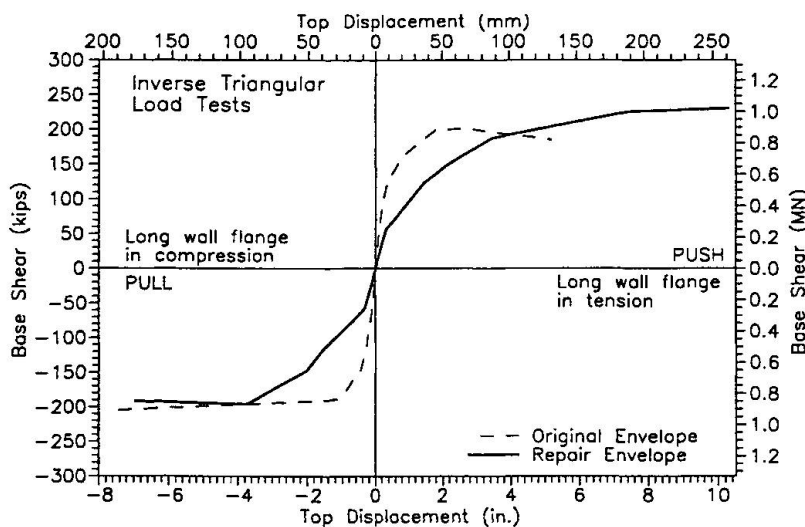


Fig. 4 Load-Displacement Envelope Comparison for Carbon Overlay Repair Test

under pseudo-dynamic simulated seismic loads to failure [5]. Subsequent to the original testing, the building was repaired by means of structural carbon overlays to the first two stories of the structural walls, (see Fig. 3b), subsequent to reconstruction of the crushed wall toes with polymer concrete.

The load-deflection envelopes for the original and the retest of the five-story building, (see Fig. 4), show that a single layer of carbon fabric overlay [$t = 1.25$ mm, predominately horizontal woven carbon fabric, (12 k toe AS4), with epoxy resin matrix], applied on each side of the structural walls with two layers in the toe regions, contributed significantly to doubling the inelastic deformation capacity. Measured shear deformations in the overlaid wall panels were reduced to half the shear deformations in the original five-story building test. Detailed information of the repair and retrofit installation and seismic response data can be found in [5].

For out-of-plane wall retrofitting the key design aspects are (1) the development of the overlay material in regions of high moment gradients, and (2) the potential for buckling and delamination of the thin and stiff overlays on the compression side of the flexural member. Detailed research data and corresponding design guidelines for both of these areas are currently being developed, reviewed, and experimentally validated.

The effectiveness of the application of advanced composite wall overlays for seismic repair and retrofitting of structural wall systems can best be demonstrated by the example of a full-scale five-story reinforced masonry building, see Fig. 3, which was tested

3.3 Bridge Superstructure Strengthening

Bridge superstructure capacity deficiencies have been encountered both for increasing traffic loads and permit overload vehicles, as well as for longitudinal seismic resistance, where current seismic design philosophy requires that sufficient superstructure capacity exists to force plastic hinging into the column. Column hinging is desirable since in the column the plastic hinge region can be (1) confined by spiral reinforcement, and (2) inspected and repaired following an earthquake without superstructure closure or traffic interruptions.

On a 1/3 scale proof test model of the San Francisco Terminal Separation replacement structure design following the 1989 Loma Prieta earthquake, the concept of carbon fabric soffit overlays was explored [6], see Fig. 5.

Only two layers of each nominally 0.56 mm thick carbon overlays with fibers along the bridge axis were applied. The effectiveness of strain transfer from the soffit reinforcement to the carbon overlay is depicted in Fig. 6, which shows for the indicated soffit location both, the reinforcement strains before and after the overlay application, as well as the recorded strains in the carbon fabric overlay. Premature joint failure of the cap/column connection prevented a full development of a plastic column hinge and with it a complete verification of the carbon overlay strengthening concept.

However, the strain transfer shown in Fig. 6, as well as measured carbon overlay strains of over 1500 $\mu\epsilon$ at other locations clearly showed the

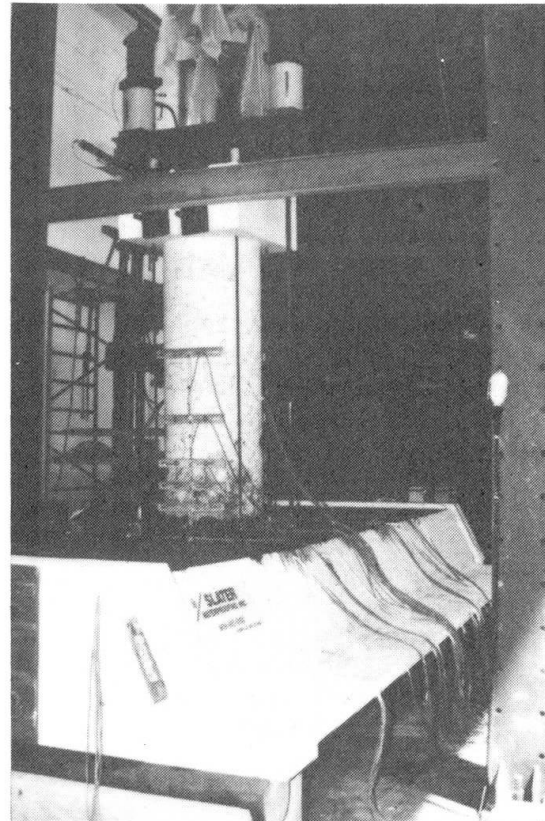


Fig. 5 Bridge Superstructure Strengthening with Soffit Carbon Overlay

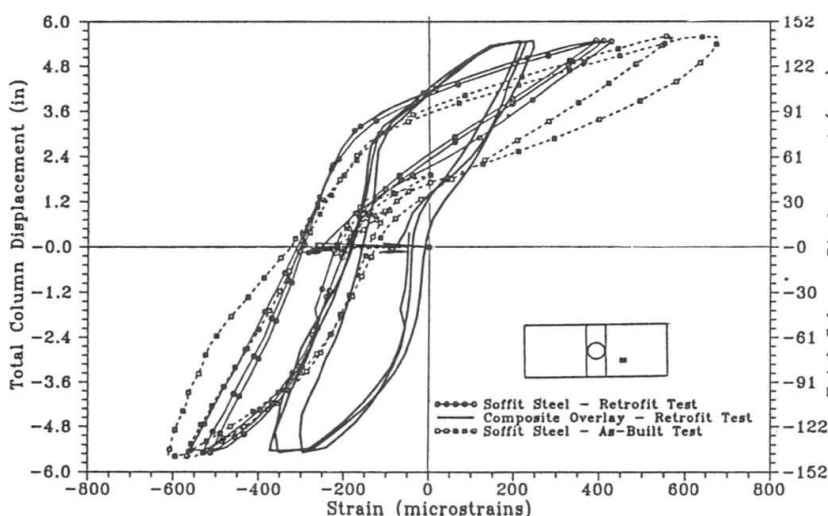


Fig. 6 Strain Comparison of Soffit Strains With and Without Carbon Overlay

contribution of the advanced composite overlay strengthening to the superstructure capacity. Buckling of the thin carbon overlay in front of the compression toe of the column, installation and quality assurance procedures, as well as design guidelines, still need to be developed prior to field applications.

In general, in all of the above described tests where hand lay-up installation of advanced composite overlays was used, significant variability in overlay thickness was observed. Thus, for a strength or stiffness based design approach nominal and not measured thicknesses and mechanical properties as verified by coupon tests need to be employed. Alternatively, the



resin or matrix system with its low mechanical characteristics is only used to locate the fiber, and the entire design is strictly based on fiber properties and number of layers of woven or stitched composite fabric without reference to the matrix or overlay thickness.

4. CONCLUSIONS

Aging and deterioration, design and detailing of existing concrete structures, as well as substandard seismic designed and detailed structures, require the rapid development of new rehabilitation technologies. Polymer matrix composites or advanced composite materials have shown high potential for structural effectiveness in rehabilitating existing concrete structures by means of thin jackets or overlays. The structural effectiveness in terms of strengthening and/or seismic retrofitting was demonstrated on numerous large or full-scale laboratory tests on building and bridge systems.

For some of these rehabilitation applications for advanced composites such as column retrofitting and in-plane structural wall strengthening, complete structural design guidelines have been developed, whereas other applications such as flexural strengthening of unreinforced walls and bridge superstructure strengthening with soffit overlays have been demonstrated in principle but detailed design guidelines do not yet exist.

In general, additional research and development is needed to address quality control issues for the application and curing of in-situ composite applications, as well as aging and durability characteristics in the civil environment. Furthermore, accidental loads such as fire, impact and subsequent repairability need to be addressed prior to the formulation of general advanced composites rehabilitation technology guidelines. All of the above issues are currently addressed under an Advanced Research Projects Agency (ARPA) Technology Reinvestment Project (TRP) research program in coordination with Caltrans and the Federal Highway Administration to provide the scientific basis for the application of advanced composites rehabilitation technology of existing concrete structures.

5. REFERENCES

- [1] "ADVANCED Composite Materials in Bridges and Structures," edited by K.W. Naele and P. Labossiere, Canadian Society for Civil Engineers, Montreal, Canada, 1992.
- [2] MEIER, U., DEURING, M., and G. SCHWEGLER, "Strengthening of Structures with CFRP Laminates, Research and Applications in Switzerland," Proceedings, 1st International Conference on Advanced Composite Materials in Bridges and Structures, Sherbrooke, Quebec, 1992.
- [3] PRIESTLEY, M.J.N., F. SEIBLE, and Y.H. CHAI, "Design Guidelines for Assessment, Retrofit and Repair of Bridges for Seismic Performance," University of California, San Diego, Structural Systems Research Project, Report No. SSRP-92/01, August 1992.
- [4] SEIBLE, F., HEGEMIER, G., PRIESTLEY, M.J.N., INNAMORATO, D., WEEKS, J., and POLICELLI, F., "Carbon Fiber Jacket Retrofit Test of Circular Shear Bridge Column, CRC-2", University of California, San Diego, Structural Systems, Advanced Composites Technology Transfer Consortium, Report No. ACTT-94/02, September 1994.
- [5] WEEKS, J., SEIBLE, F., HEGEMIER, G., and KINGSLEY, G., "The U.S.-TCCMAR Full-Scale 5-Story Masonry Research Building Test: Part V - Repair and Retest," University of California, San Diego, Structural Systems Research Project, Rpt No. SSRP-94/05, Jan. 1994.
- [6] DOWELL, R., BURGUEÑO, R., SEIBLE, F., PRIESTLEY, M.J.N., and MARI, A., "The Terminal Separation Replacement Structure Proof test and Retrofit Test," University of California, San Diego, Structural Systems Research Project, Rpt No. SSRP-94/15, Oct. 1994.